Electronic supplementary information (ESI) **Revised**

Theoretical (DFT, GIAO-NMR, NICS) Study of Carbocations $(M+H)^+$, Dications (M^{2+}) and Dianions (M^{2-}) from Dihydro-dicyclopenta[*ef*,*kl*]heptalene (Dihydro-azupyrene), Dihydro-dicyclohepta[*ed*,*gh*]pentalene, and Related Bridged [14]annulenes

Takao Okazaki[a,b] and Kenneth K. Laali*[b]

[a)] Department of Energy and Hydrocarbon Chemistry, Kyoto University, Kyoto, Japan

[b)] Department of Chemistry, Kent State University, Kent, OH 44242, USA

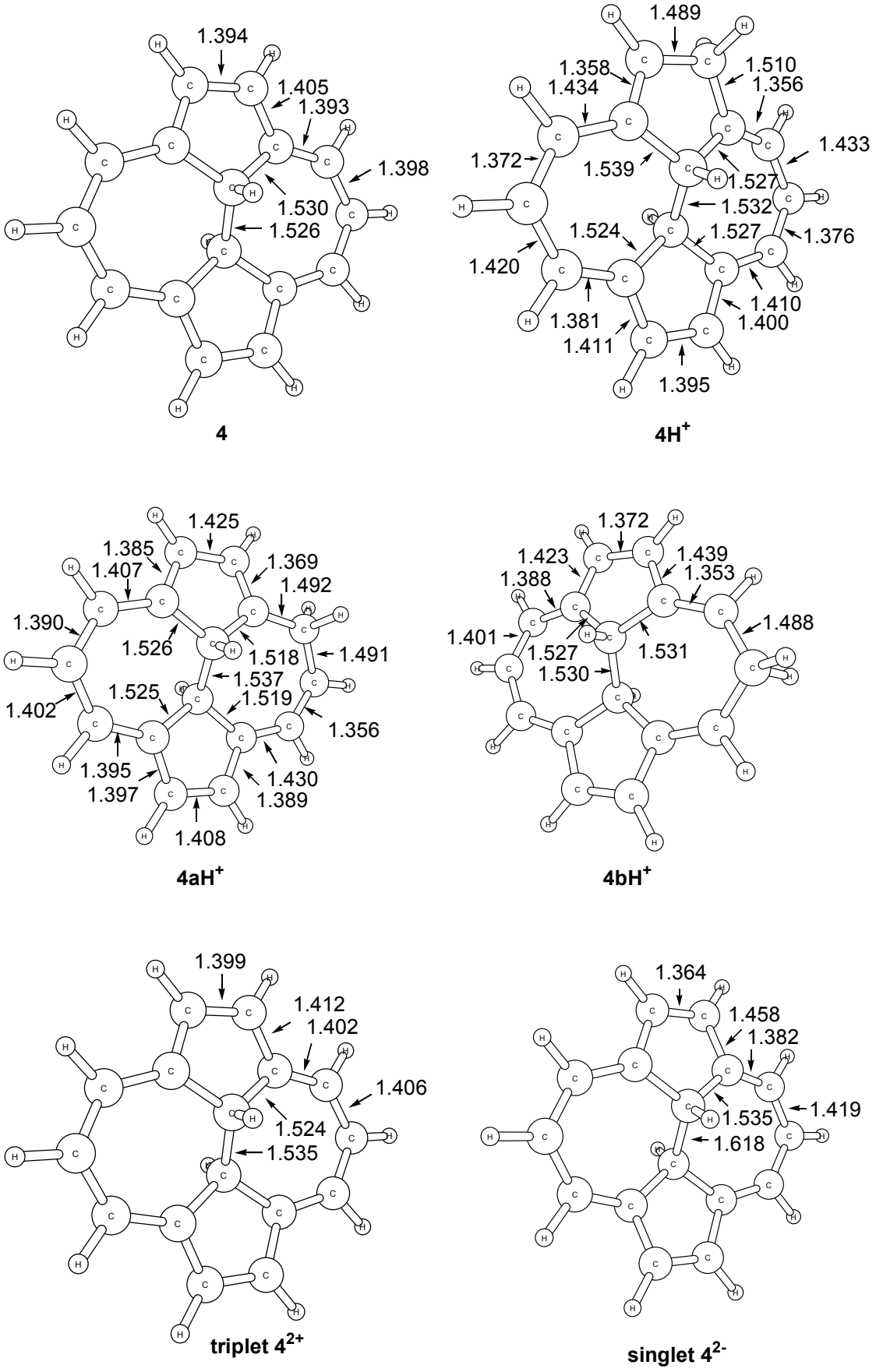

Fig S1. Optimized geometries for **4**, **4H**$^+$, **4aH**$^+$, **4bH**$^+$, triplet **4**$^{2+}$, and singlet **4**$^{2-}$ at B3LYP/6-31G(d) level (bond length, Å).

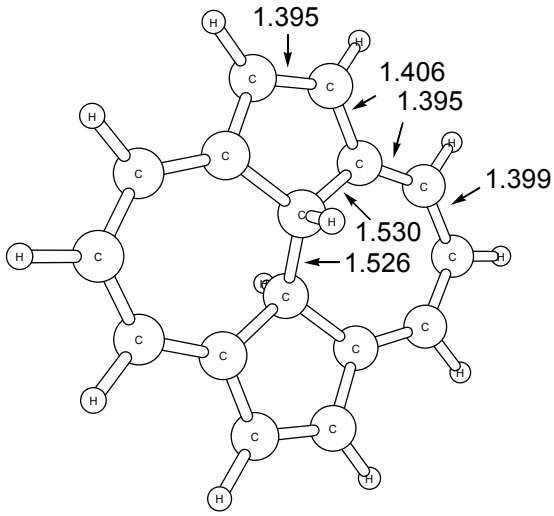

4 [B3LYP/6-31+G(d,p)]

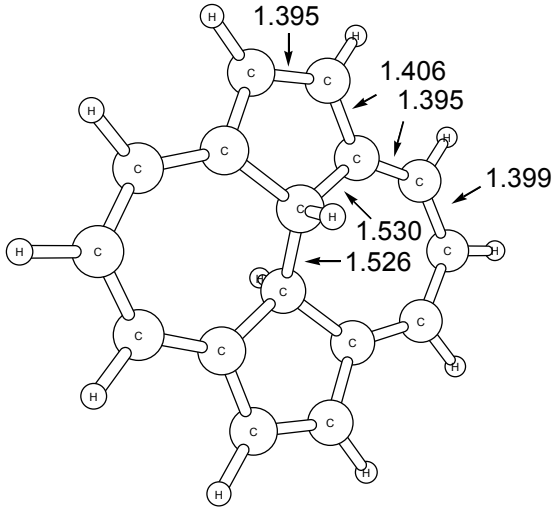

4 [B3LYP/6-31++G(d,p)]

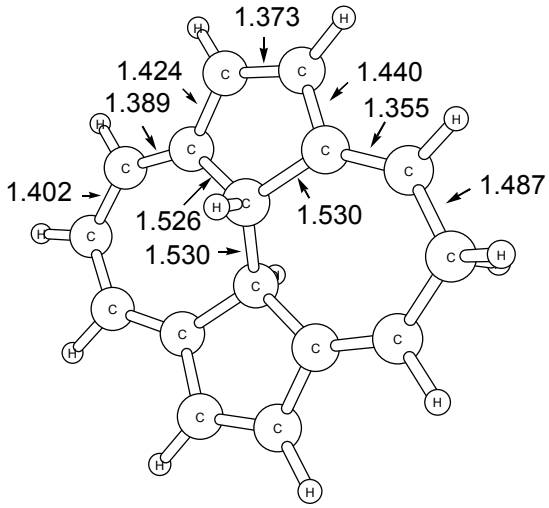

4bH$^+$ [B3LYP/6-31+G(d,p)]

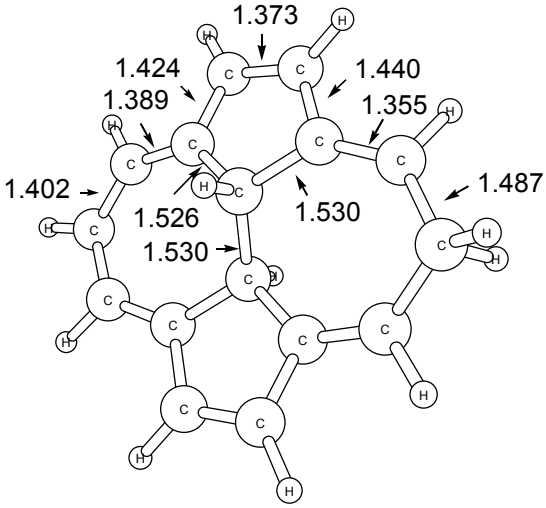

4bH$^+$ [B3LYP/6-31++G(d,p)]

Fig S1a. Optimized geometries for **4**, **4bH**$^+$, triplet **4**$^{2+}$, and singlet **4**$^{2-}$ at B3LYP/6-31+G(d,p) and B3LYP/6-31++G(d,p) levels (bond length, Å).

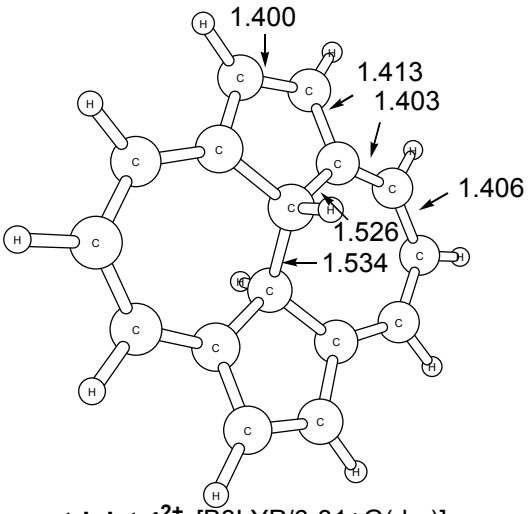

triplet 4^{2+} [B3LYP/6-31+G(d,p)]

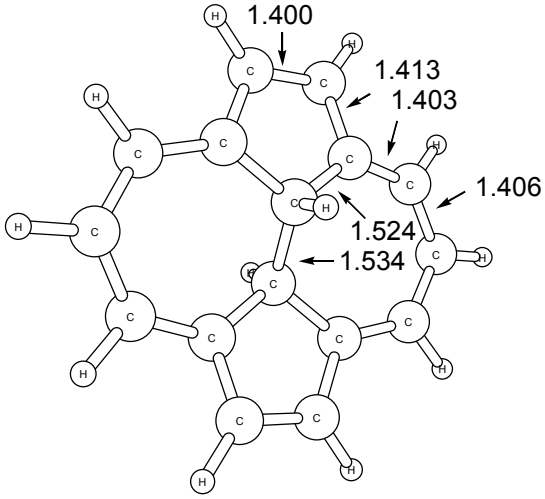

triplet 4^{2+} [B3LYP/6-31++G(d,p)]

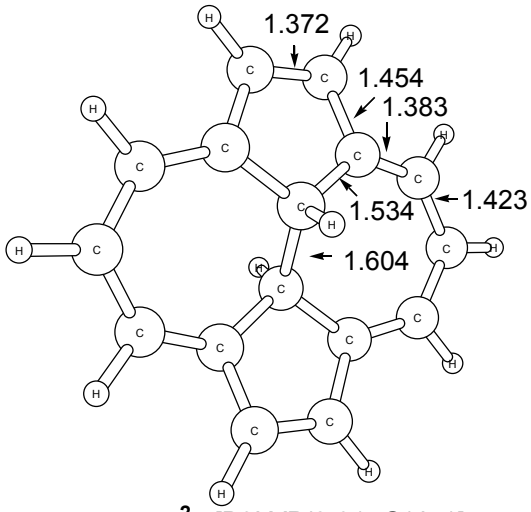

singlet 4^{2-} [B3LYP/6-31+G(d,p)]

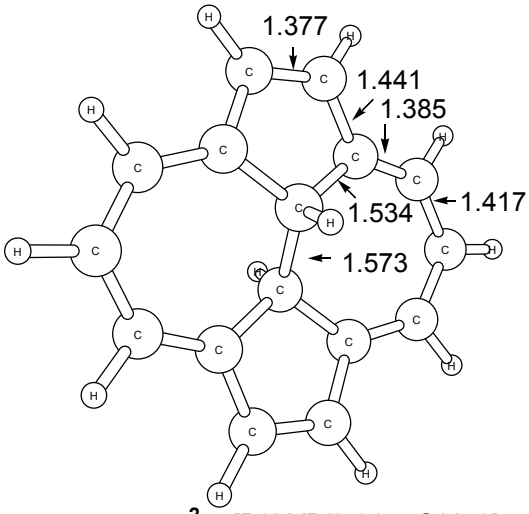

singlet 4^{2-} [B3LYP/6-31++G(d,p)]

Fig S1a (contined).

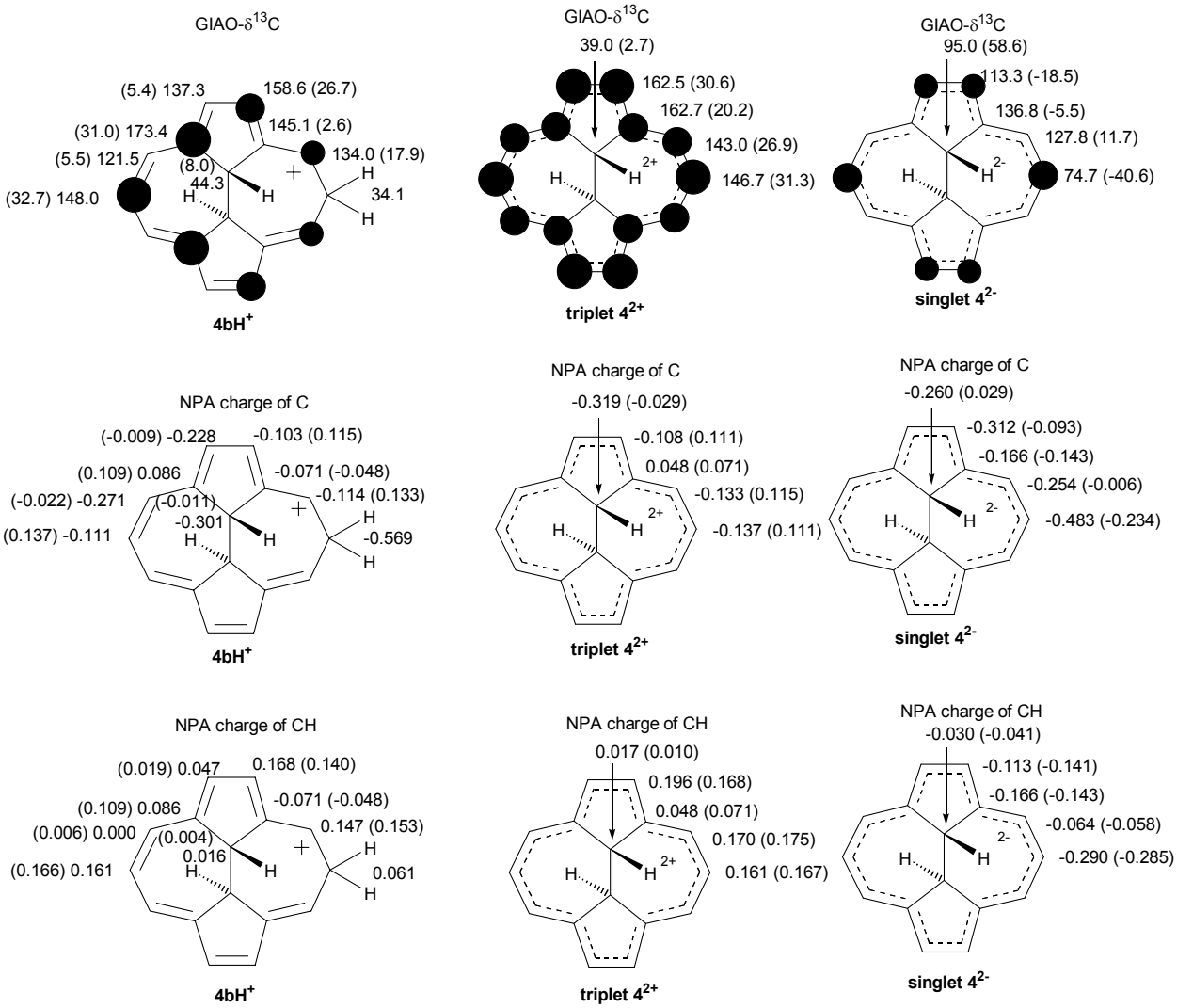

Fig S1b. Computed ^{13}C NMR chemical shifts, NPA-derived carbon charges, and NPA-derived overall charges over CH units for **4bH**$^{+}$, triplet **4**$^{2+}$, and singlet **4**$^{2-}$ ($\Delta\delta$ ^{13}C's and Δcharges relative to **4** in parentheses) at B3LYP/6-31+G(d,p) level. [*Dark circles are roughly proportional to the magnitude of* $\Delta\delta^{13}$*Cs (positive/downfield for the carbocations/dication and negative/upfield for the dianion) ; threshold was set to 10 ppm].*

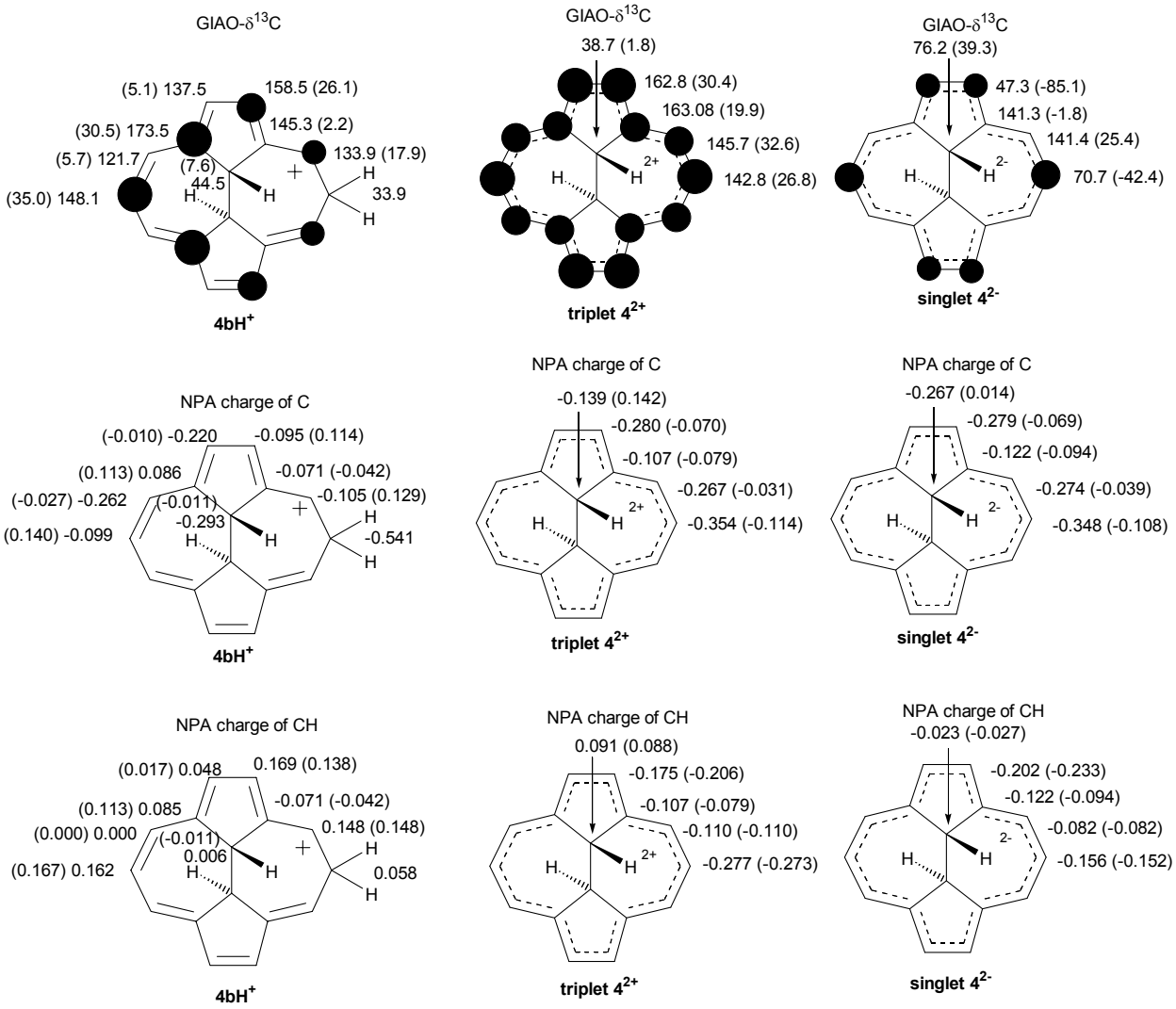

Fig S1c. Computed ^{13}C NMR chemical shifts, NPA-derived carbon charges, and NPA-derived overall charges over CH units for **4bH**$^{+}$, triplet **4**$^{2+}$, and singlet **4**$^{2-}$ ($\Delta\delta$ ^{13}C's and Δcharges relative to **4** in parentheses) at B3LYP/6-31++G(d,p) level. [*Dark circles are roughly proportional to the magnitude of* $\Delta\delta^{13}$*Cs (positive/downfield for the carbocations/dication and negative/upfield for the dianion); threshold was set to 10 ppm].*

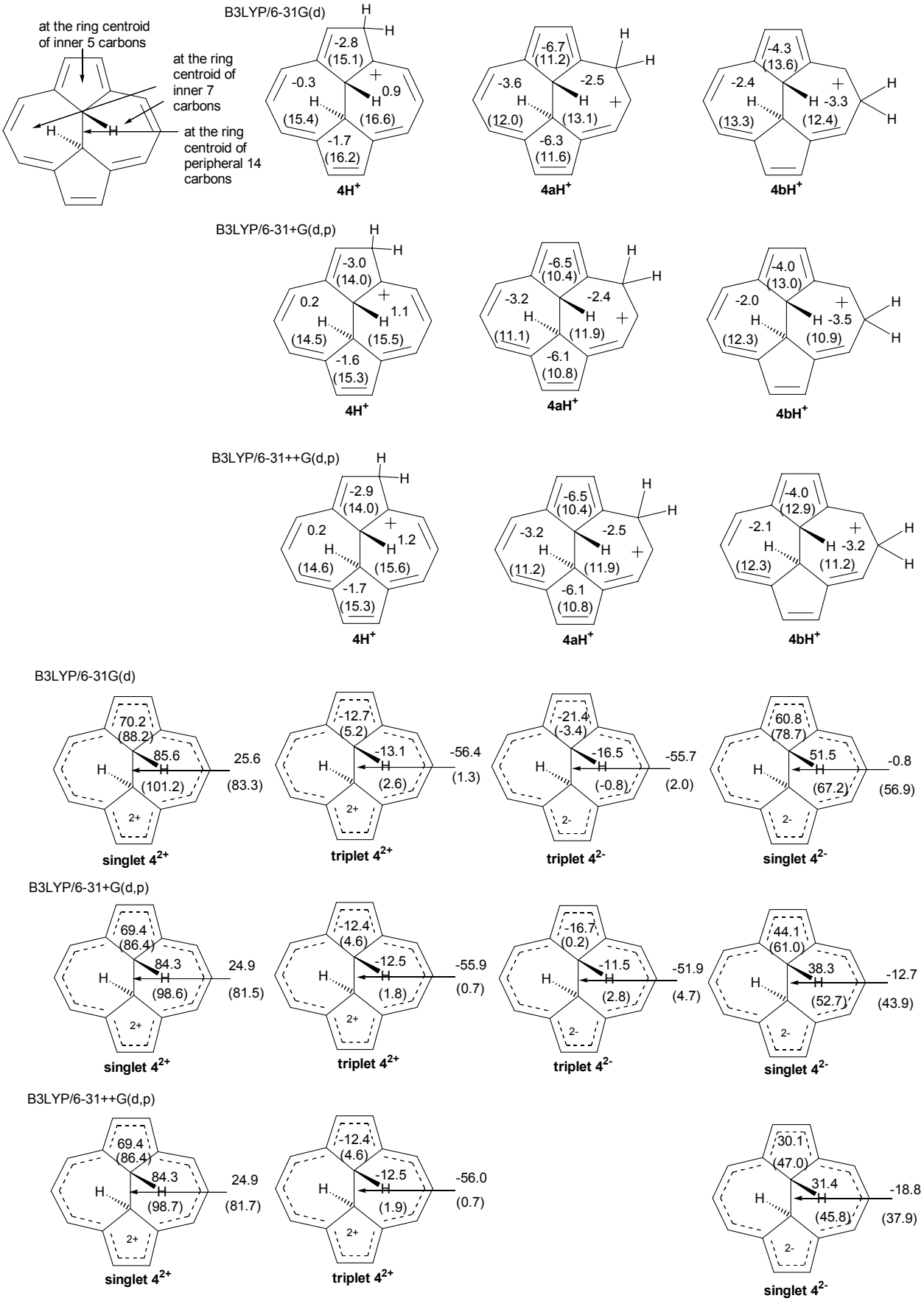

Fig S2. NICS values for $\mathbf{4H^+}$, $\mathbf{4aH^+}$, $\mathbf{4bH^+}$, $\mathbf{4^{2+}}$, and $\mathbf{4^{2-}}$ at B3LYP/6-31G(d), 6-31+G(d,p), or 6-31++G(d,p) level (ΔNICS values relative to those of **4** in parentheses).

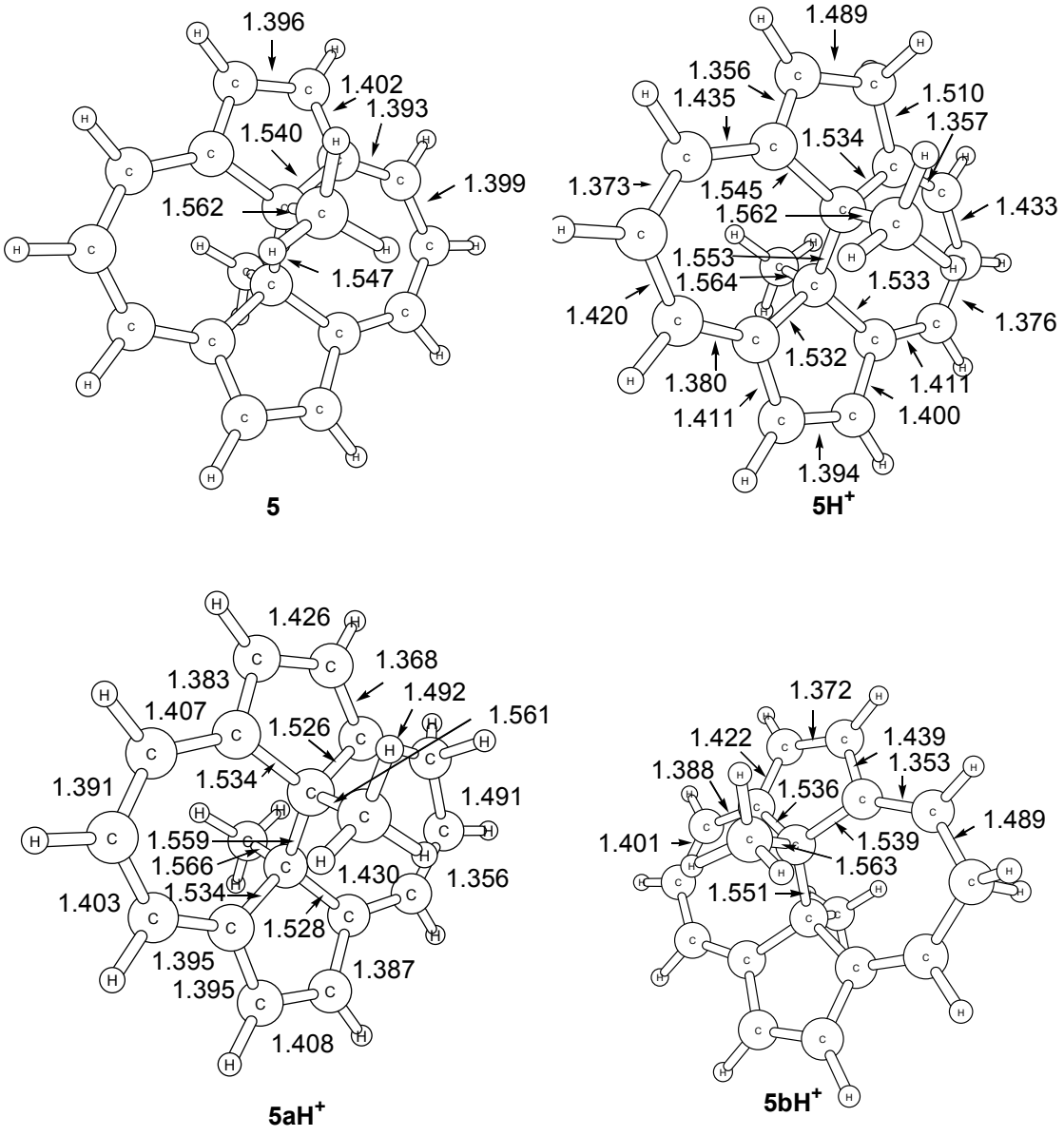

Fig S3. B3LYP/6-31G(d) optimized geometries for **5**, $\mathbf{5H^+}$, $\mathbf{5aH^+}$, $\mathbf{5bH^+}$, $\mathbf{5^{2+}}$, and $\mathbf{5^{2-}}$ (bond length, Å).

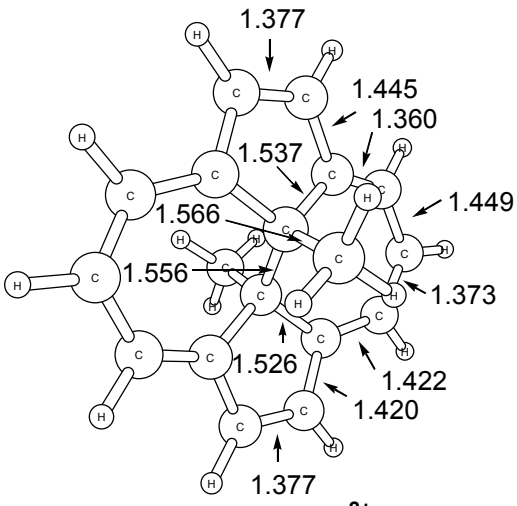

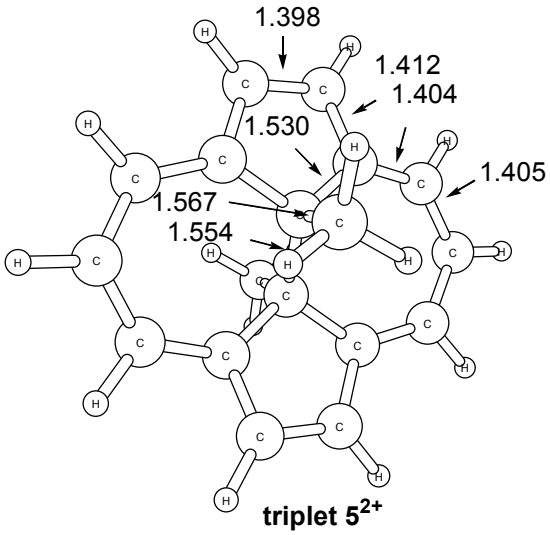

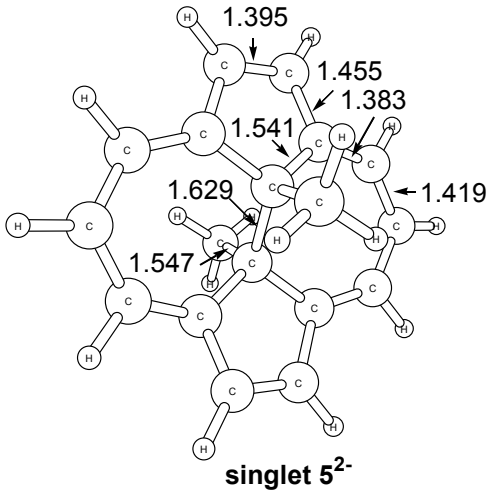

Fig S3 (continued).

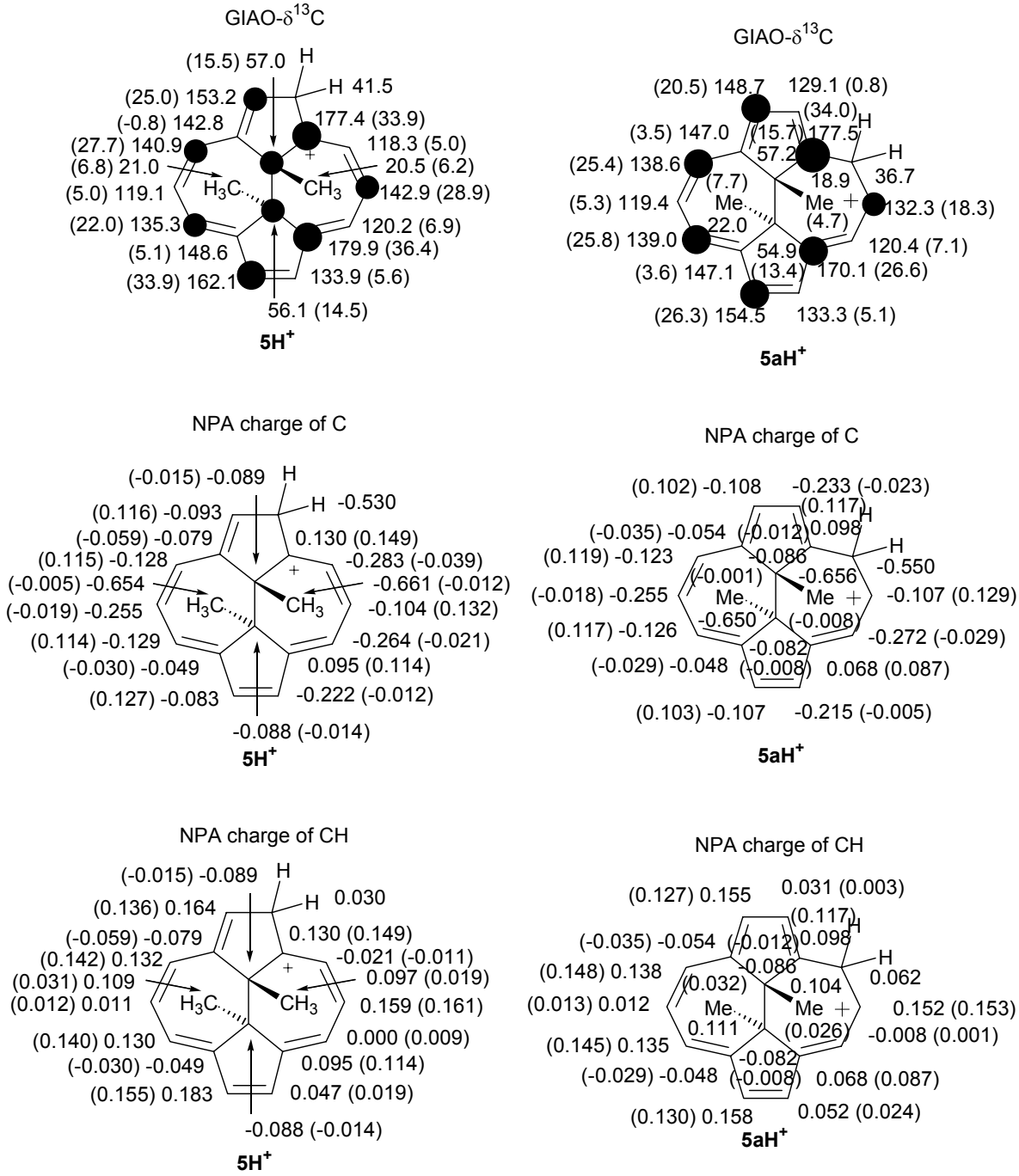

Fig S4. Computed ^{13}C NMR chemical shifts, NPA-derived carbon charges, and NPA-derived overall charges over CH units for **5H**$^{+}$, **5aH**$^{+}$, **5bH**$^{+}$, **5**$^{2+}$, and **5**$^{2-}$ at B3LYP/6-31G(d) level ($\Delta\delta$ ^{13}C's and Δcharges relative to **5** in parentheses). [*Dark circles are roughly proportional to the magnitude of* $\Delta\delta^{13}$*Cs (positive/downfield for the carbocations/dication and negative/upfield for the dianion); threshold was set to 10 ppm].*

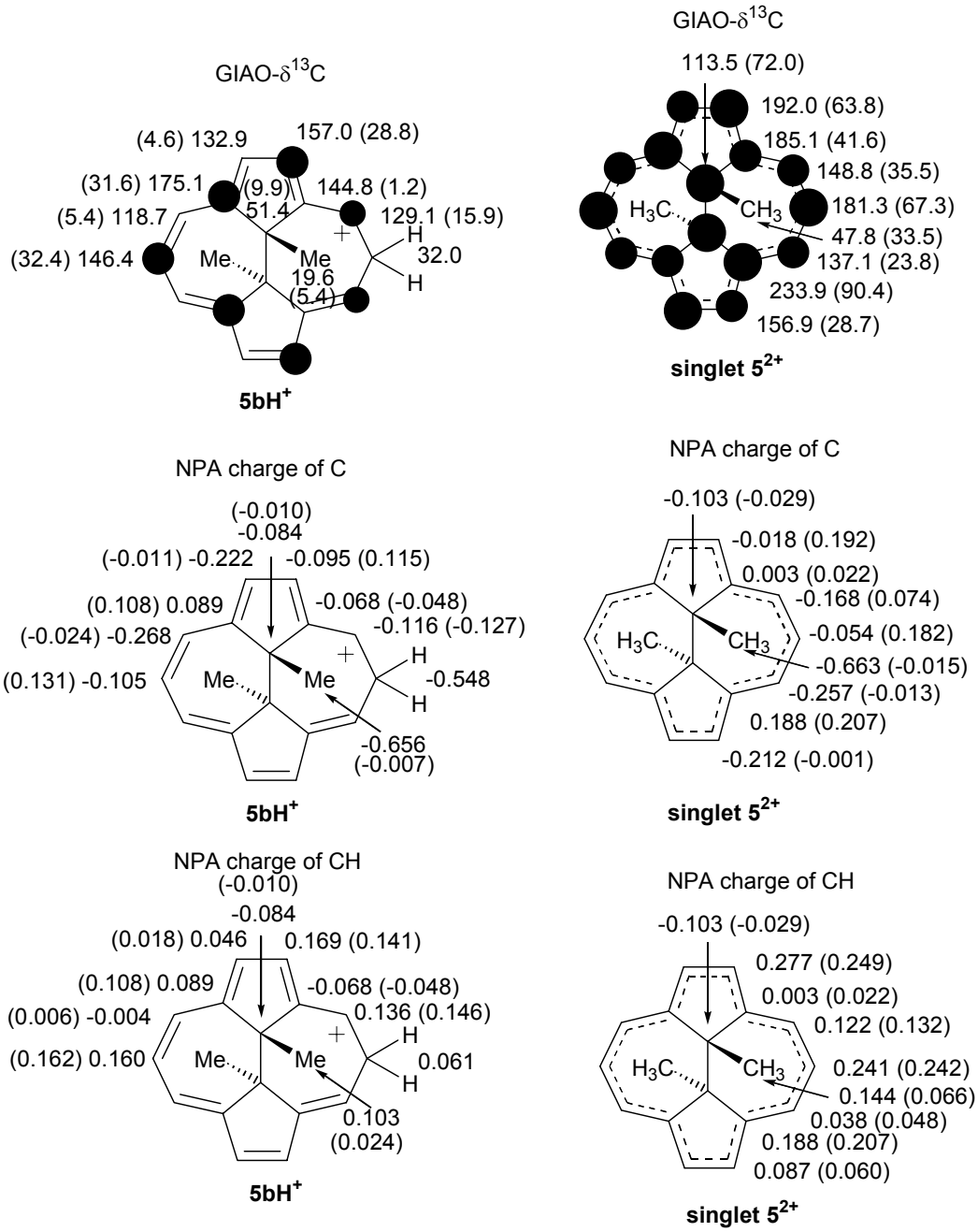

Fig S4 (continued).

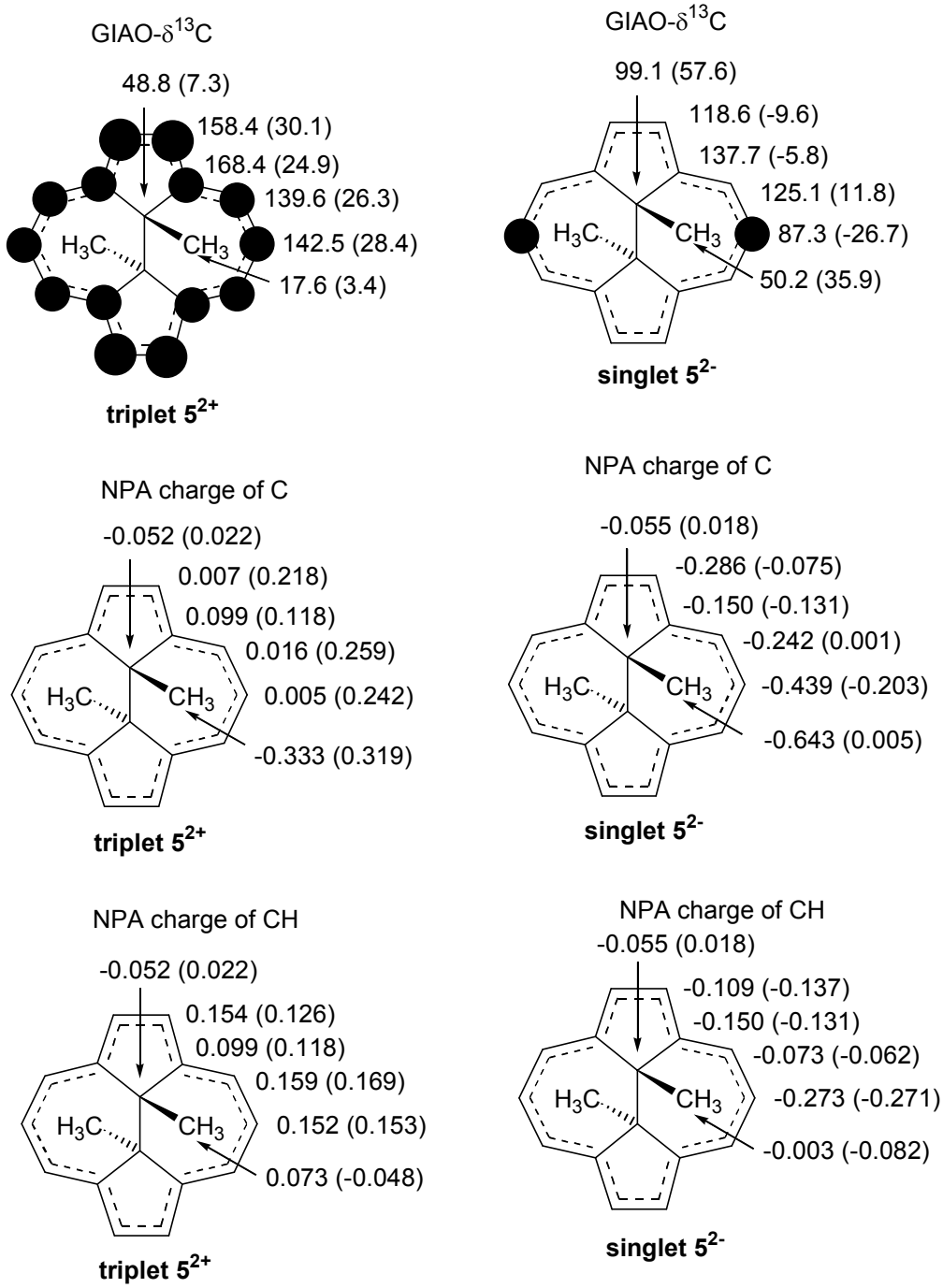

Fig S4 (continued).

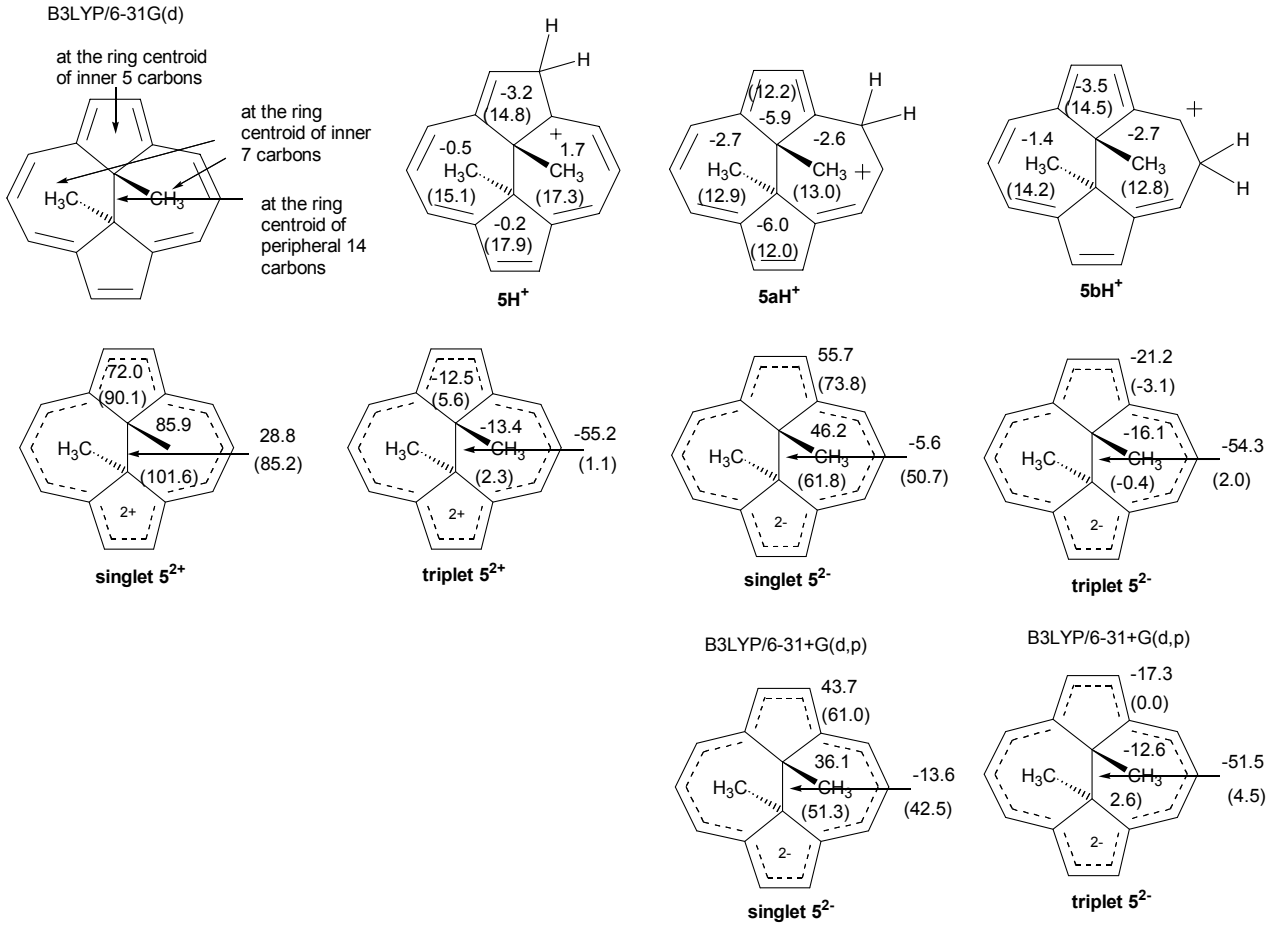

Fig S5. NICS values for $\mathbf{5H^+}$, $\mathbf{5aH^+}$, $\mathbf{5bH^+}$, $\mathbf{5^{2+}}$, and $\mathbf{5^{2-}}$ at B3LYP/6-31G(d) or 6-31+G(d,p) level (ΔNICS values relative to those of **5** in parentheses).

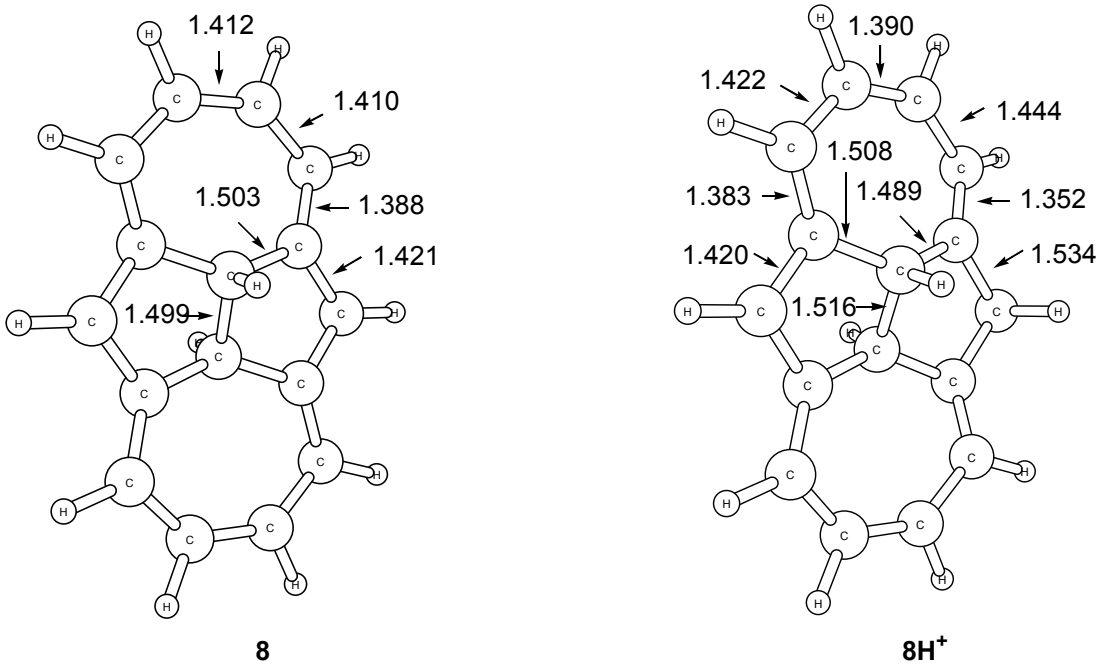

Fig S6. B3LYP/6-31G(d) optimized geometries for **8**, $\mathbf{8H^+}$, triplet $\mathbf{8^{2+}}$, and singlet $\mathbf{8^{2-}}$ (bond length, Å).

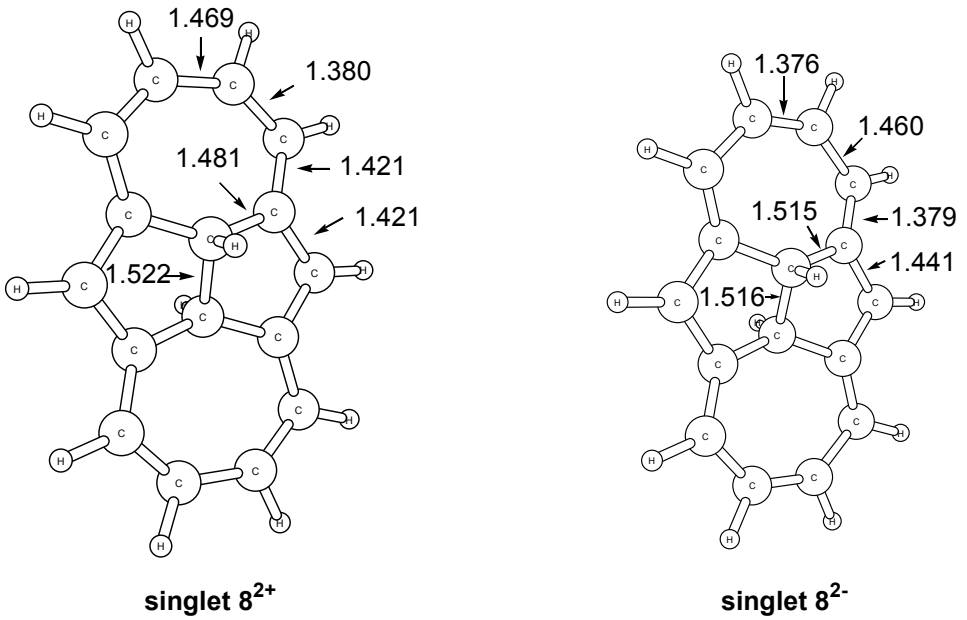

Fig S6 (continued).

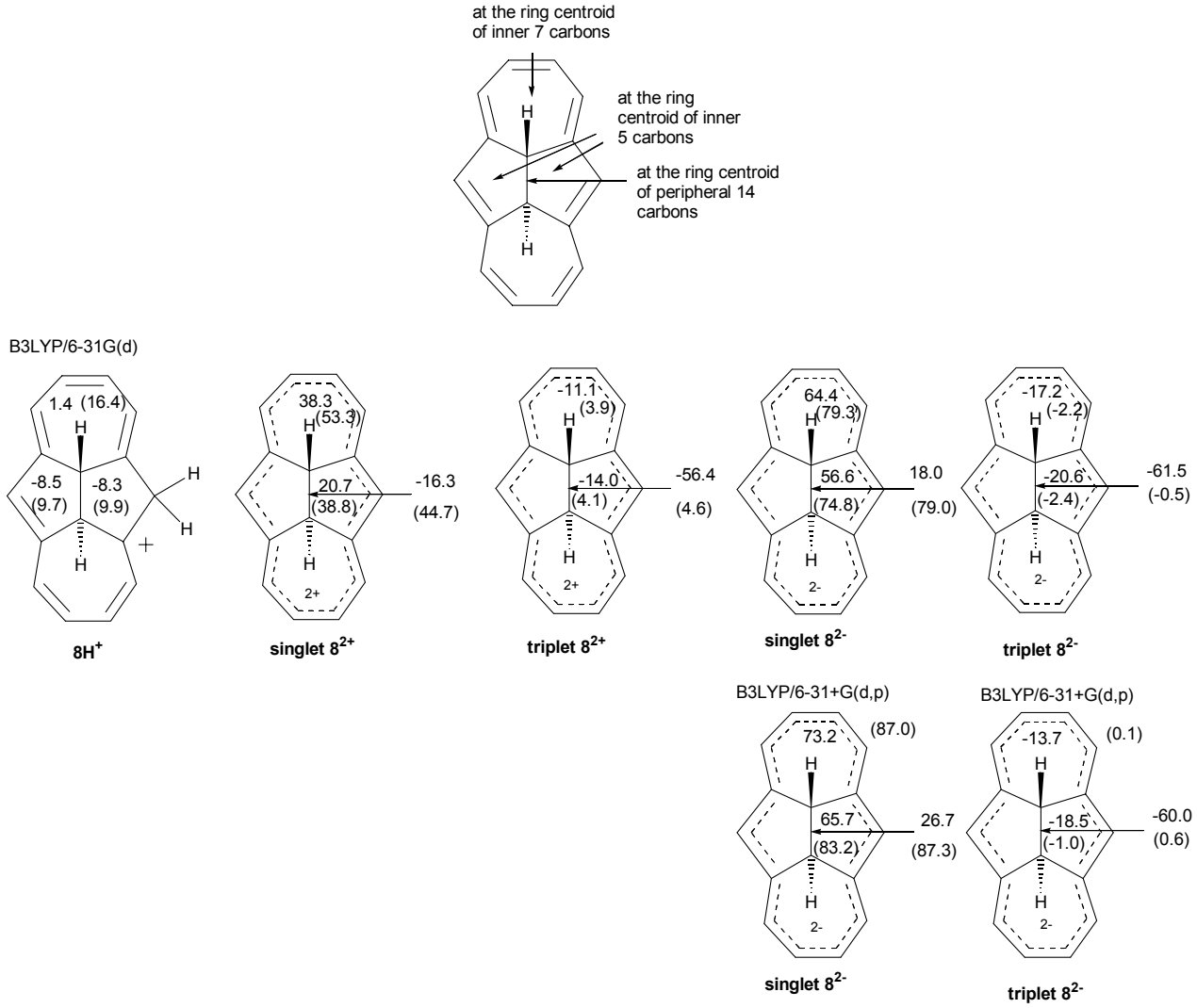

Fig S7. NICS values for $\mathbf{8H^+}$, $\mathbf{8^{2+}}$, and $\mathbf{8^{2-}}$ at B3LYP/6-31G(d) or 6-31+G(d,p) level (ΔNICS values relative to those of **8** in parentheses).

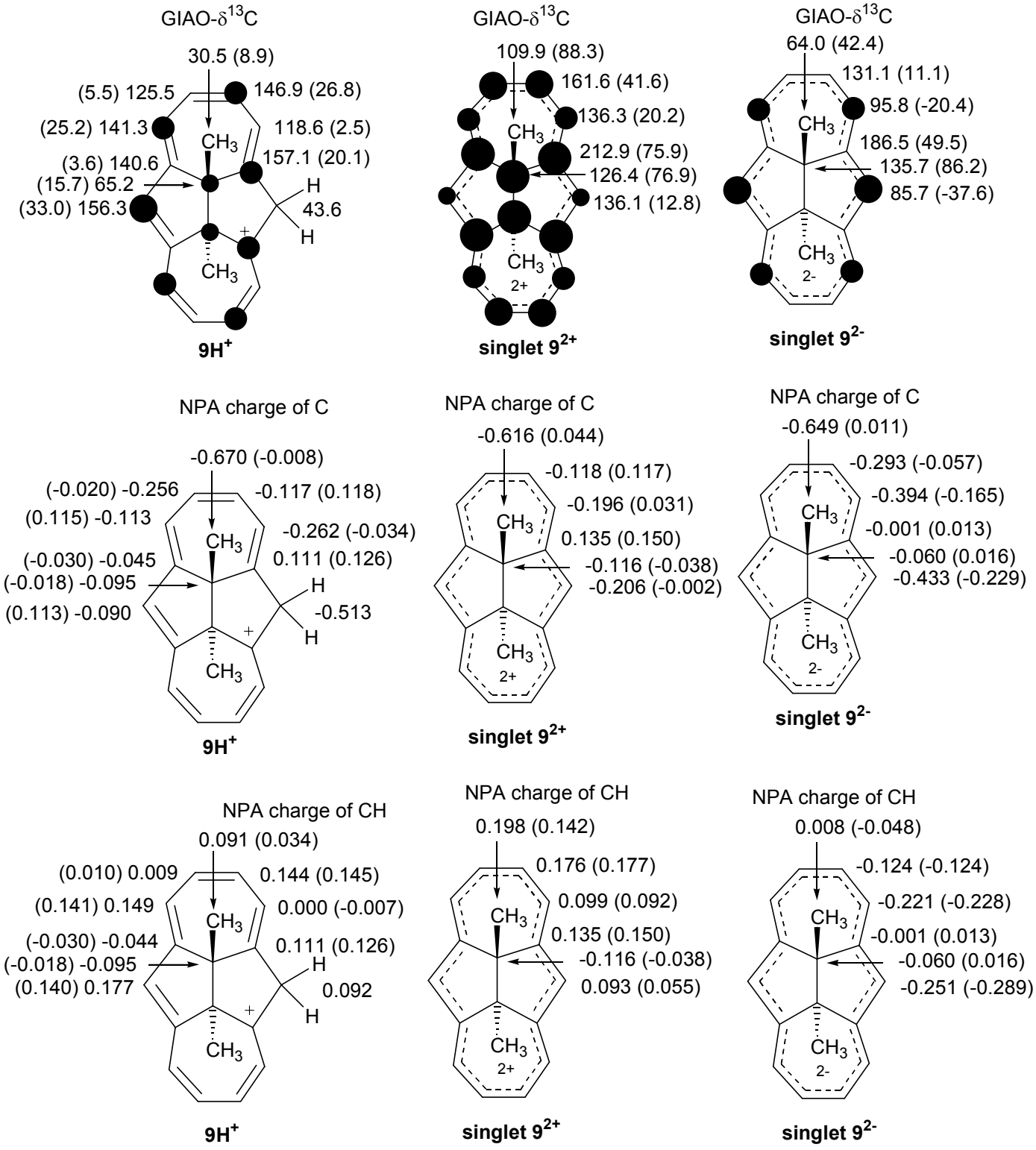

Fig S8. Computed ^{13}C NMR chemical shifts, NPA-derived carbon charges, and NPA-derived overall charges over CH units for $\mathbf{9H^+}$, $\mathbf{9^{2+}}$, and $\mathbf{9^{2-}}$ at B3LYP/6-31G(d) level ($\Delta\delta$ ^{13}C's and Δcharges relative to **9** in parentheses). [*Dark circles are roughly proportional to the magnitude of $\Delta\delta$ ^{13}Cs (positive/downfield for the carbocations/dication and negative/upfield for the dianion); threshold was set to 10 ppm]*.

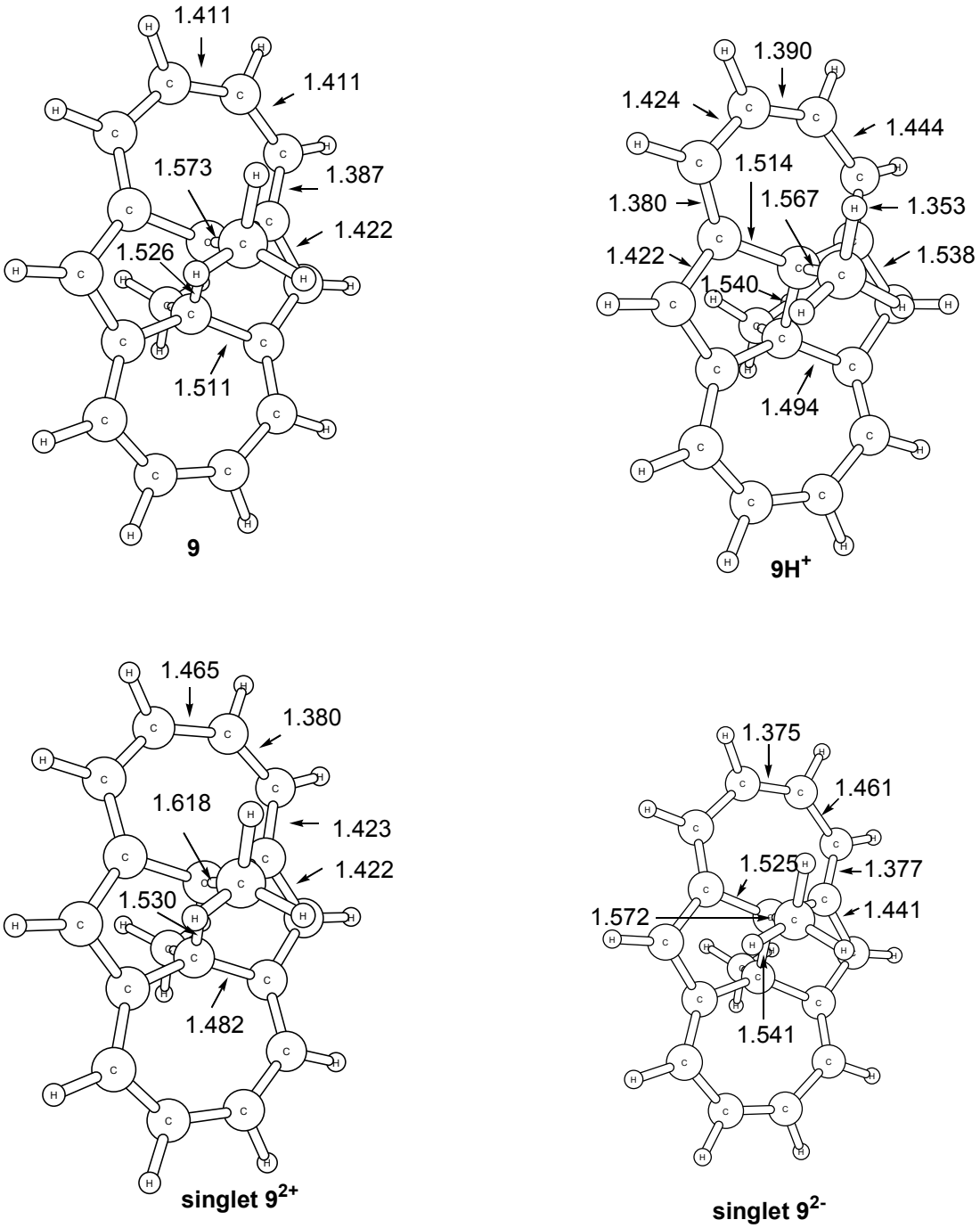

Fig S9. B3LYP/6-31G(d) optimized geometries for **9**, $\mathbf{9H^+}$, triplet $\mathbf{9^{2+}}$, and singlet $\mathbf{9^{2-}}$ (bond length, Å).

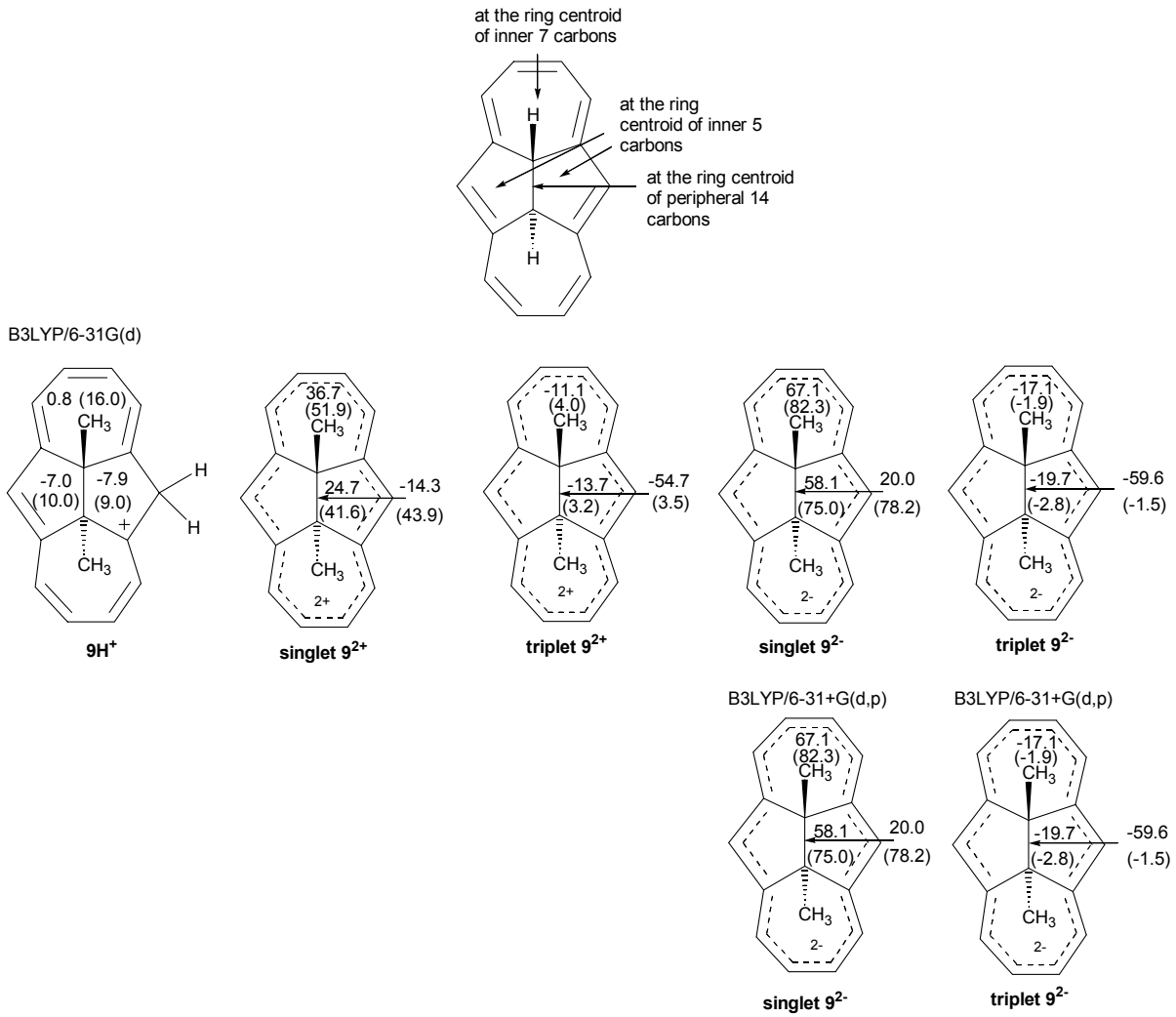

Fig S10. NICS values for $\mathbf{9H^+}$, $\mathbf{9^{2+}}$, and $\mathbf{9^{2-}}$ at B3LYP/6-31G(d) or 6-31+G(d,p) level (ΔNICS values relative to those of **9** in parentheses).

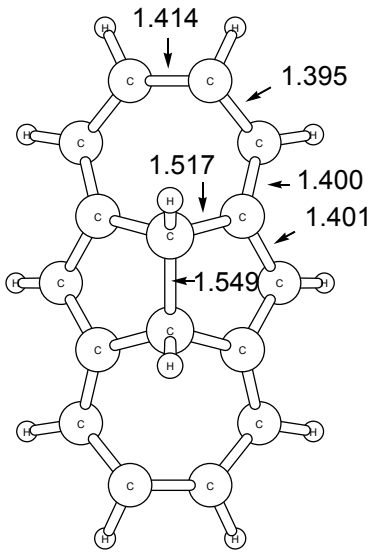

10

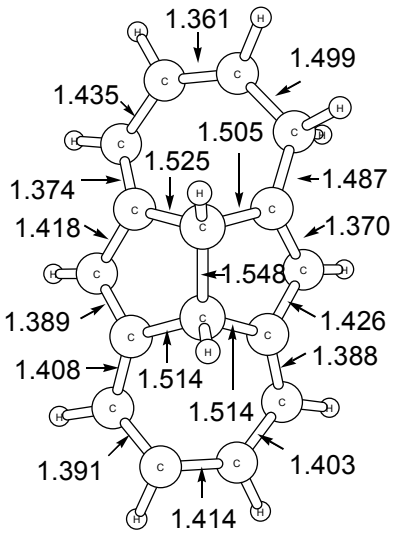

10aH^{+}

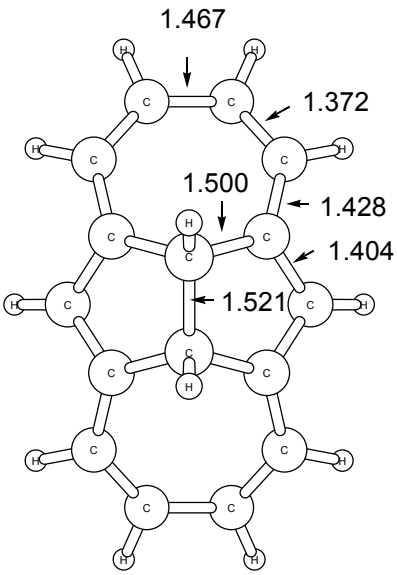

singlet 10^{2+}

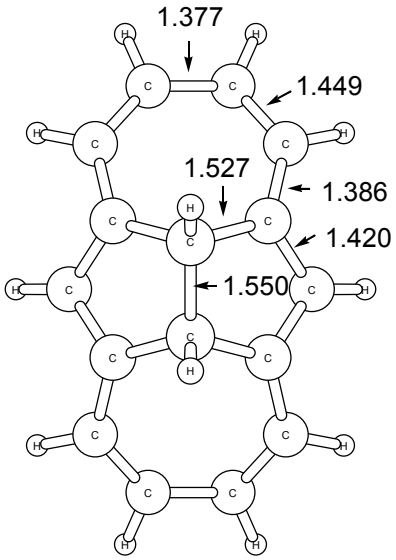

singlet 10^{2-}

Fig S11. B3LYP/6-31G(d) optimized geometries for **10**, **10aH**$^{+}$, singlet **10**$^{2+}$, and singlet **10**$^{2-}$ (bond length, Å).

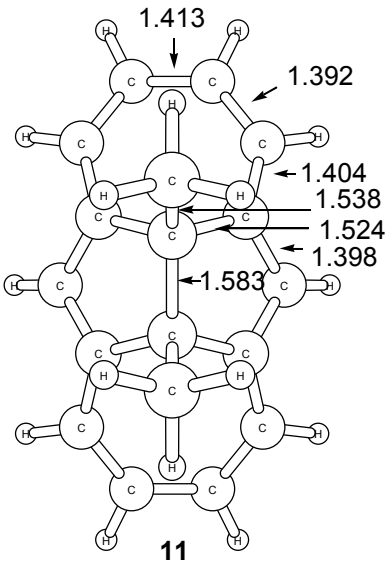

11

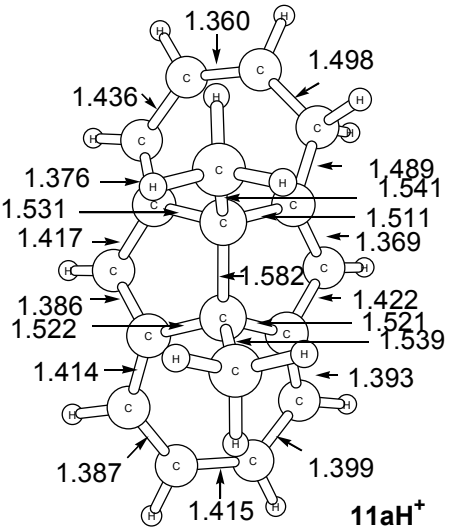

11aH$^+$

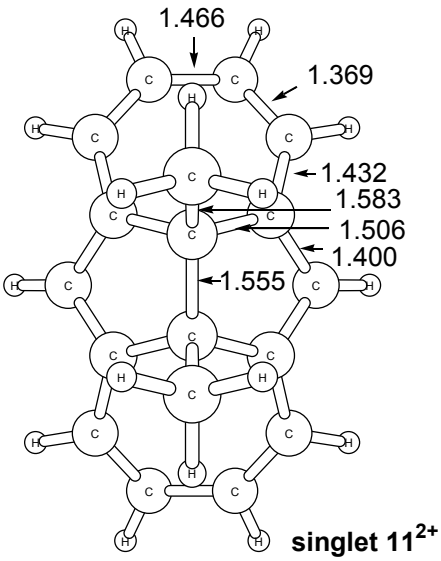

singlet 11^{2+}

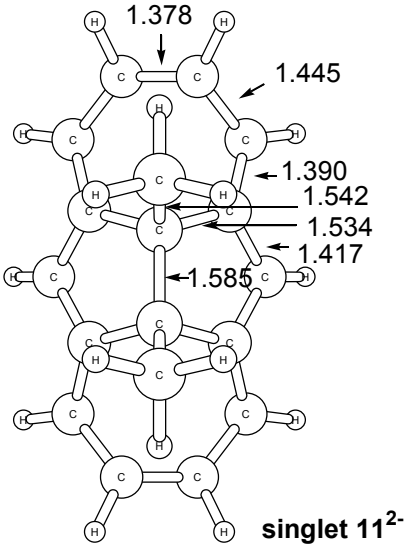

singlet 11^{2-}

X-ray structure

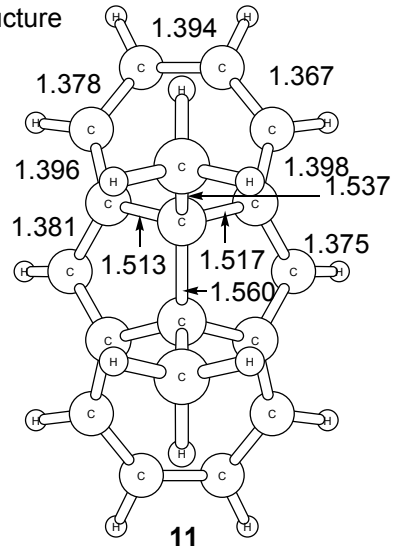

11

Fig S12. B3LYP/6-31G(d) optimized geometries for **11**, **11H**$^+$, singlet **11**$^{2+}$, and singlet **11**$^{2-}$ and X-ray structure for **11** (bond length, Å).

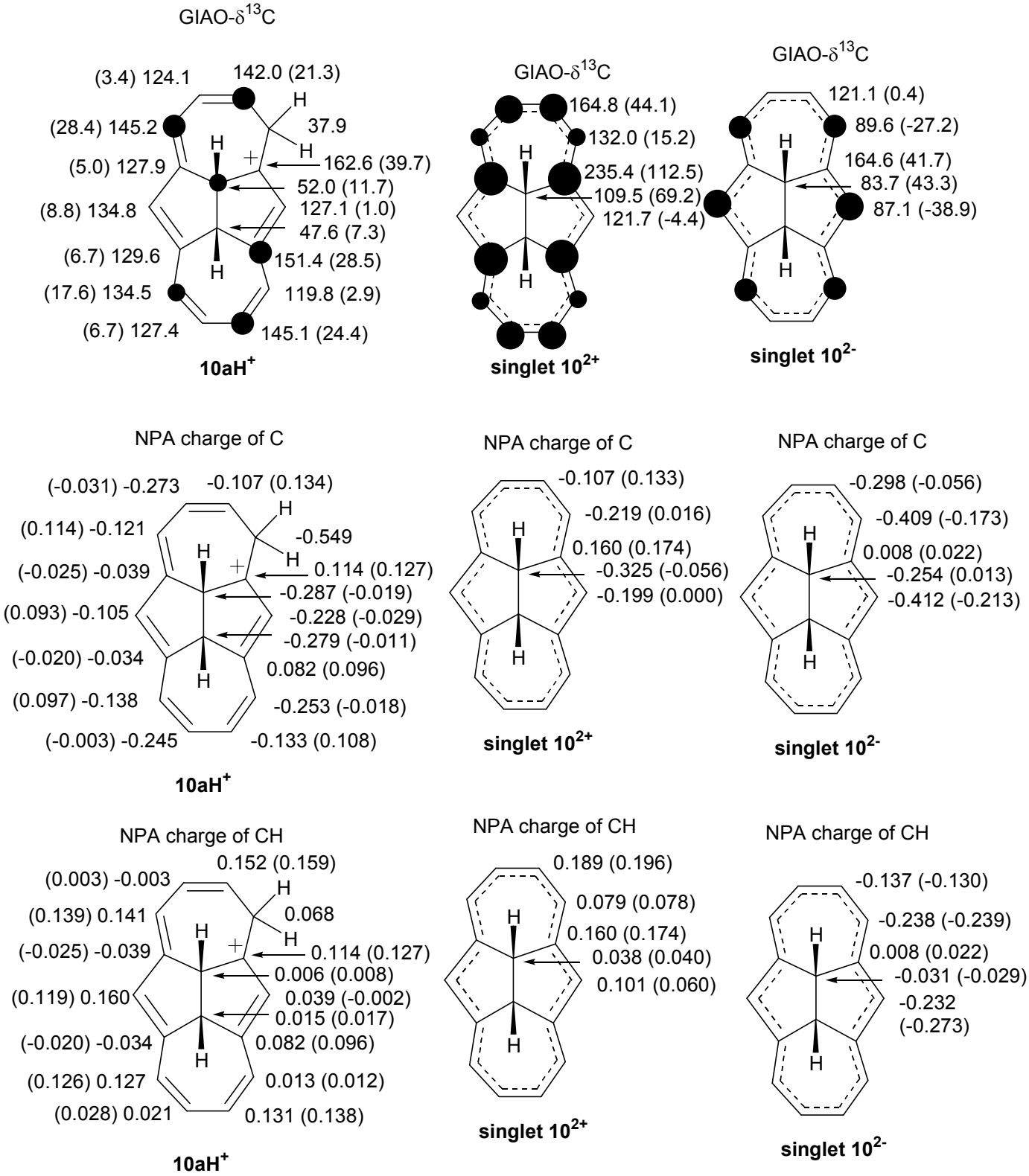

Fig S13. Computed ^{13}C NMR chemical shifts, NPA-derived carbon charges, and NPA-derived overall charges over CH units for **10aH**$^{+}$, **10**$^{2+}$, and **10**$^{2-}$ at B3LYP/6-31G(d) level ($\Delta\delta$ ^{13}C's and Δcharges relative to **10** in parentheses). [*Dark circles are roughly proportional to the magnitude of* $\Delta\delta$ ^{13}*Cs (positive/downfield for the carbocations/dication and negative/upfield for the dianion); threshold was set to 10 ppm]*.

GIAO-δ^{13}C

B3LYP/6-311++G(3df,3pd)//B3LYP/6-31G(d)

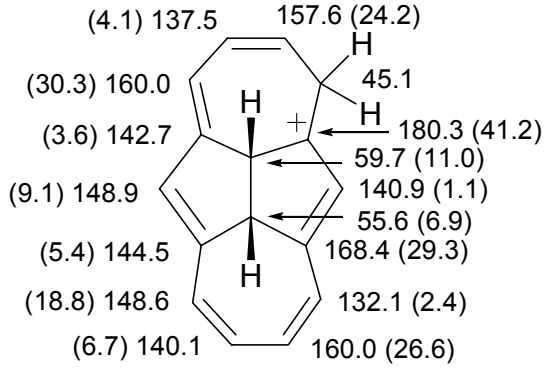

B3LYP/6-31+G(d,p)//B3LYP/6-31G(d)

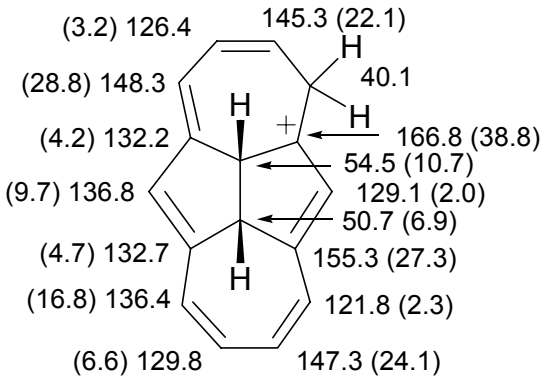

B3LYP/6-311++G(d,p)//B3LYP/6-31G(d)

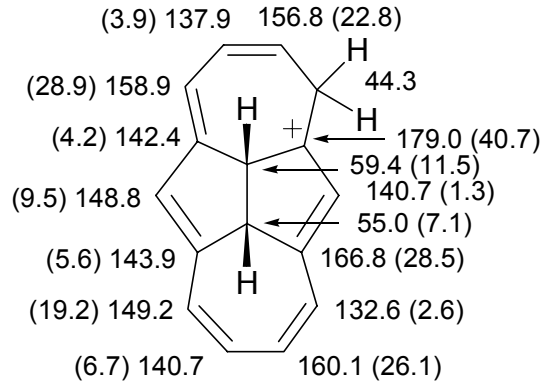

B3LYP/6-311++G(d,p)//B3LYP/6-311++G(d,p)

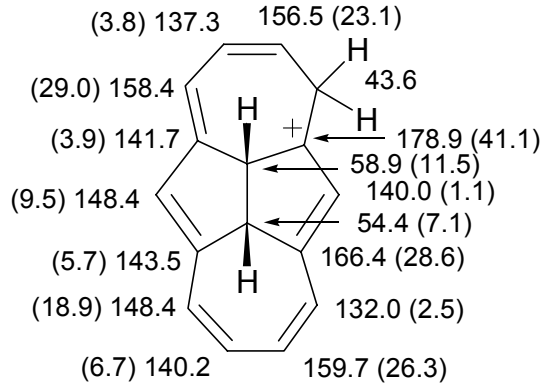

B3LYP/6-31G(d)//B3LYP/6-31G(d)

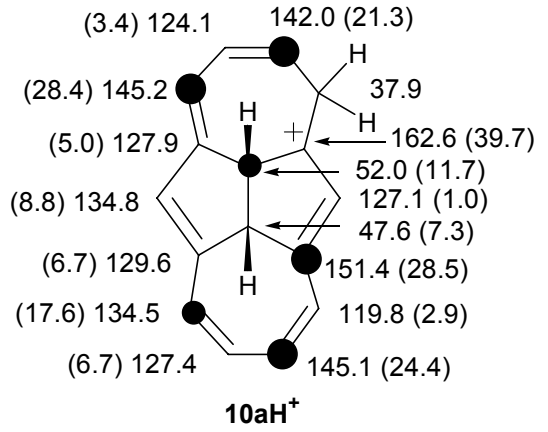

10aH$^+$

Experimental-δ^{13}C
(in superacid solution)

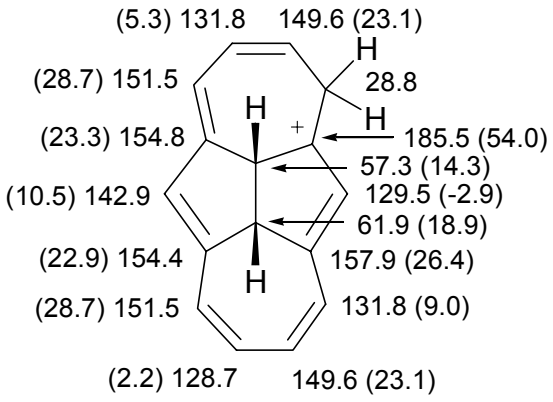

Fig S13a. Experimental (Ref 22) and computed ^{13}C NMR chemical shifts for **10aH$^+$**.

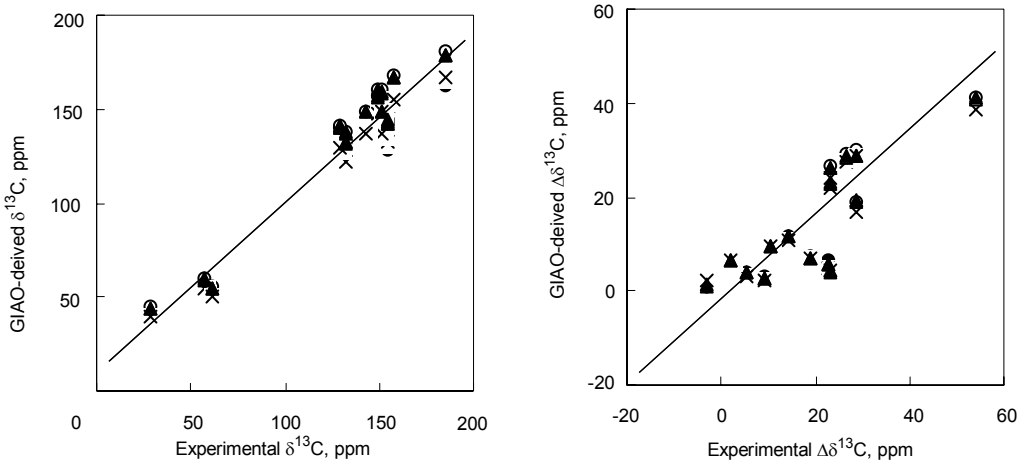

Figure S13b. Plots of experimental $\delta^{13}C$ vs GIAO-derived $\delta^{13}C$ and experimental $\Delta\delta^{13}C$ vs GIAO-derived $\Delta\delta^{13}C$ for **10aH**$^+$ by (○) B3LYP/6-31G(d)//B3LYP/6-31G(d), (●) B3LYP/6-31+G(d,p)//B3LYP/6-31G(d), (×) B3LYP/6-311++G(d,p)//B3LYP/6-31G(d), (Δ) B3LYP/6-311++G(3df,3pd)//B3LYP/6-31G(d), (▲) B3LYP/6-311++G(d,p)//B3LYP/6-311++G(d,p) .

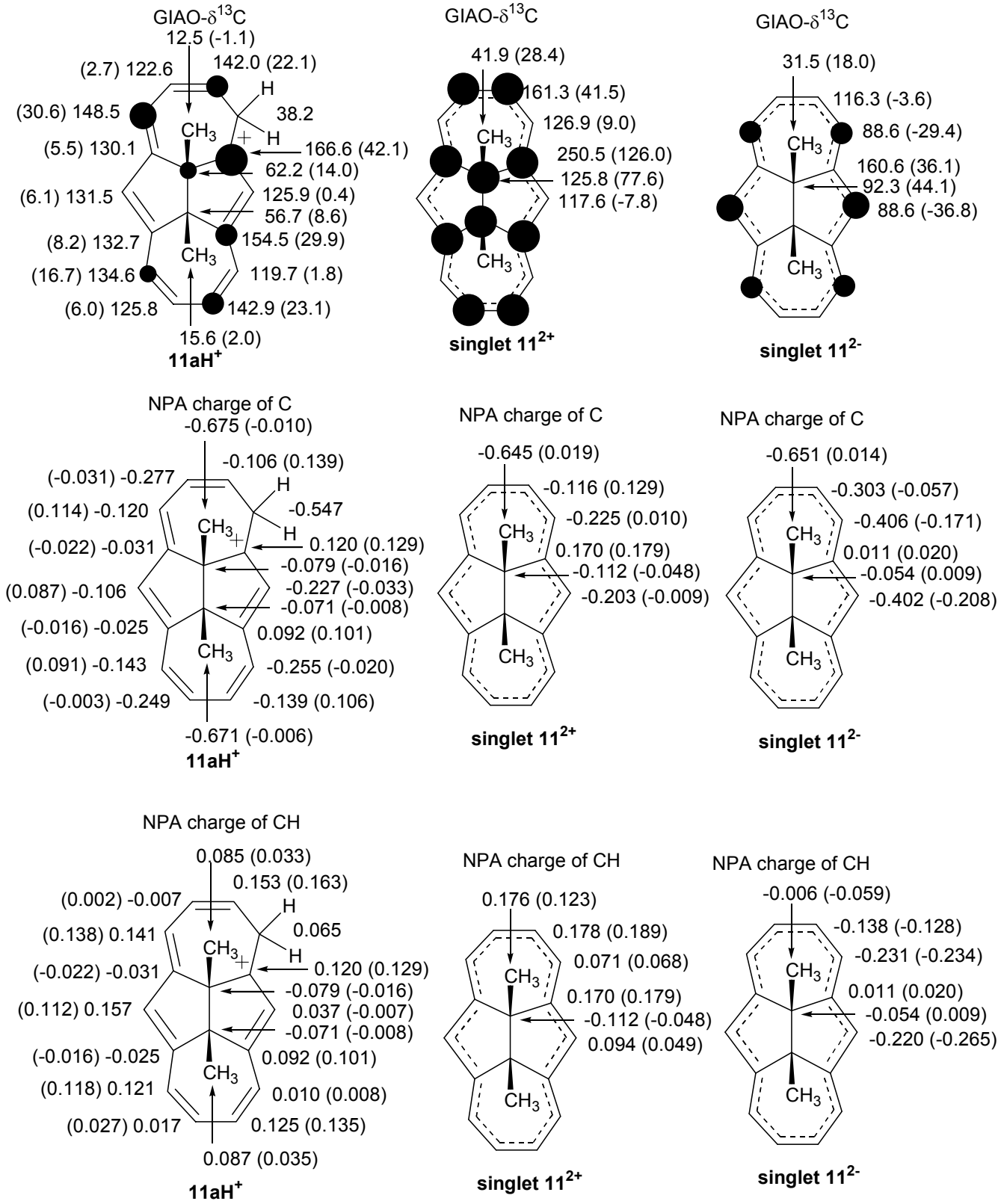

Fig S14. Computed ^{13}C NMR chemical shifts, NPA-derived carbon charges, and NPA-derived overall charges over CH units for **11aH**$^{+}$, **11**$^{2+}$, and **11**$^{2-}$ at B3LYP/6-31G(d) level ($\Delta\delta$ ^{13}C's and Δcharges relative to **11** in parentheses). [*Dark circles are roughly proportional to the magnitude of* $\Delta\delta$ ^{13}*Cs (positive/downfield for the carbocations/dication and negative/upfield for the dianion); threshold was set to 10 ppm]*.

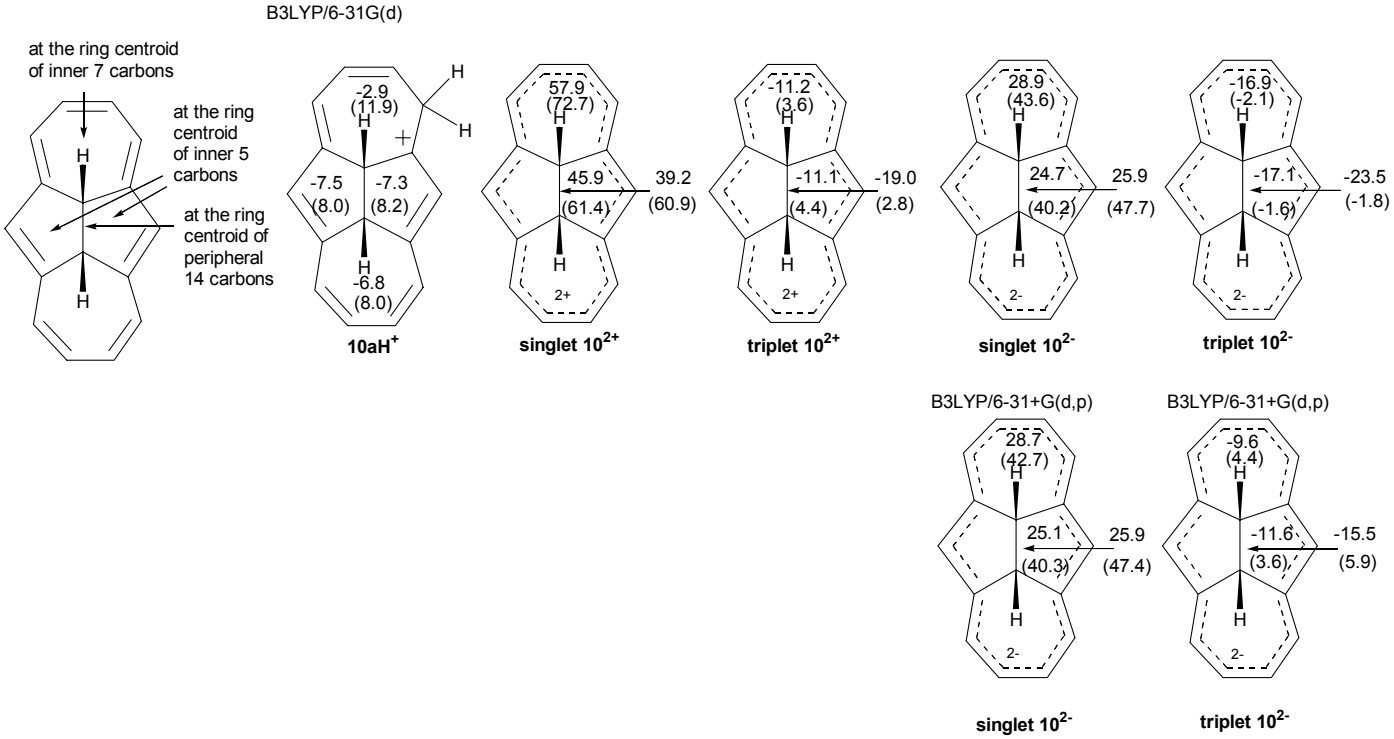

Fig S15. NICS values for **10aH**$^{+}$, **10**$^{2+}$, and **10**$^{2-}$ at B3LYP/6-31G(d) or 6-31+G(d,p) level (ΔNICS values relative to those of **10** in parentheses).

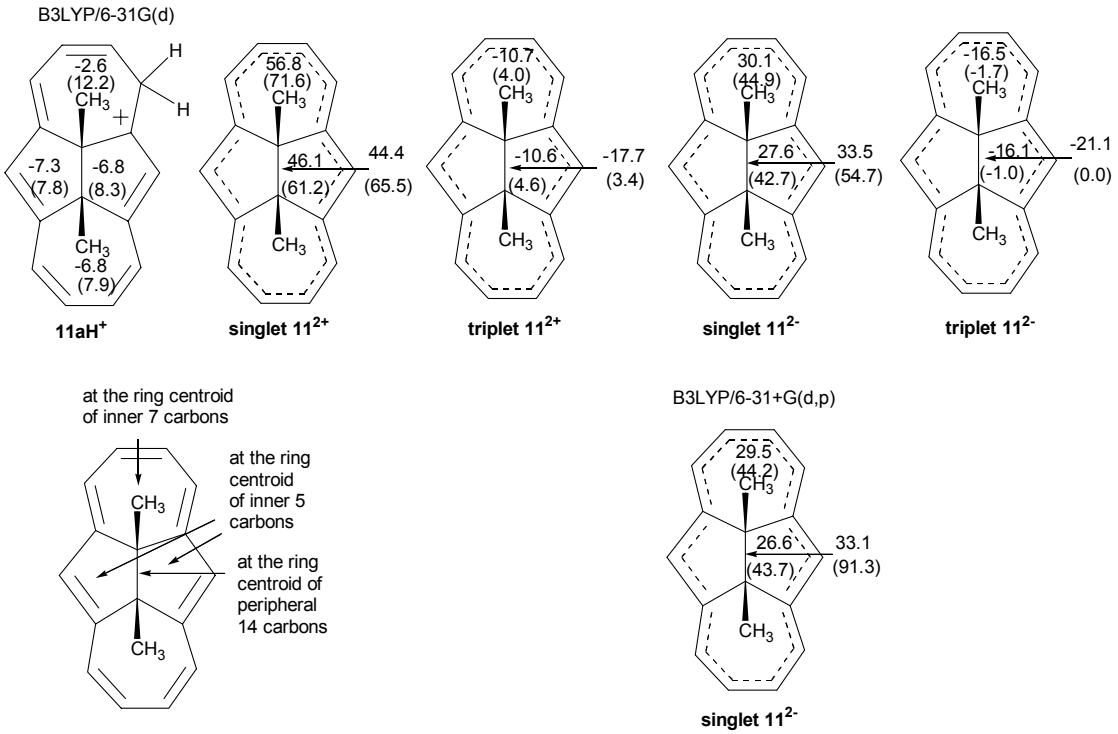

Fig S16. NICS values for **11aH**$^{+}$**, 11**$^{2+}$ and **11**$^{2-}$ at B3LYP/6-31G(d) or 6-31+G(d,p) level (ΔNICS values relative to those of **11** in parentheses).

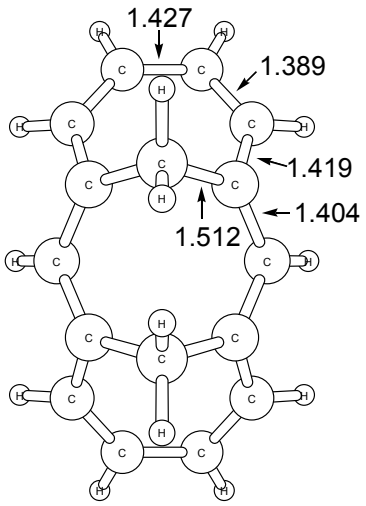

14

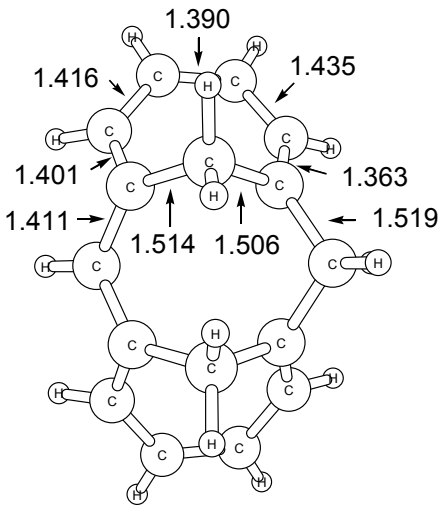

14H$^+$

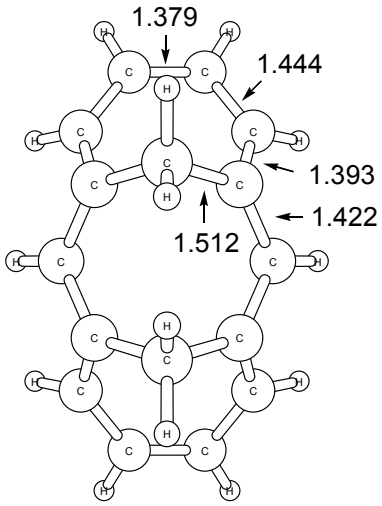

singlet 14^{2+}

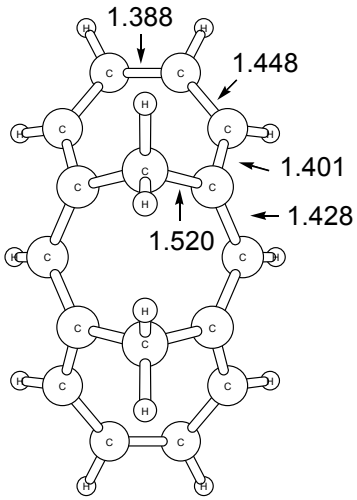

singlet 14^{2-}

X-ray structure

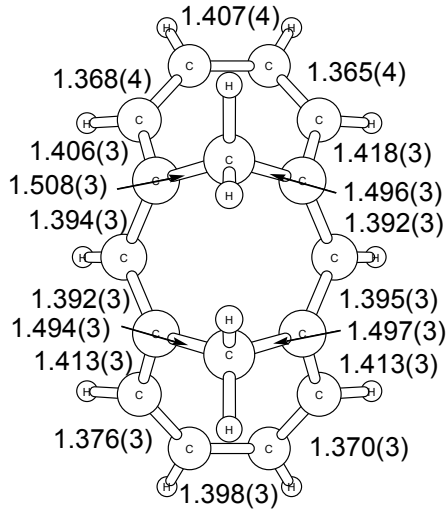

14

Fig S17. B3LYP/6-31G(d) optimized geometries for **14**, **14H**$^+$, singlet **14**$^{2+}$ and singlet **14**$^{2-}$ and X-ray structure for **14** (bond length, Å).

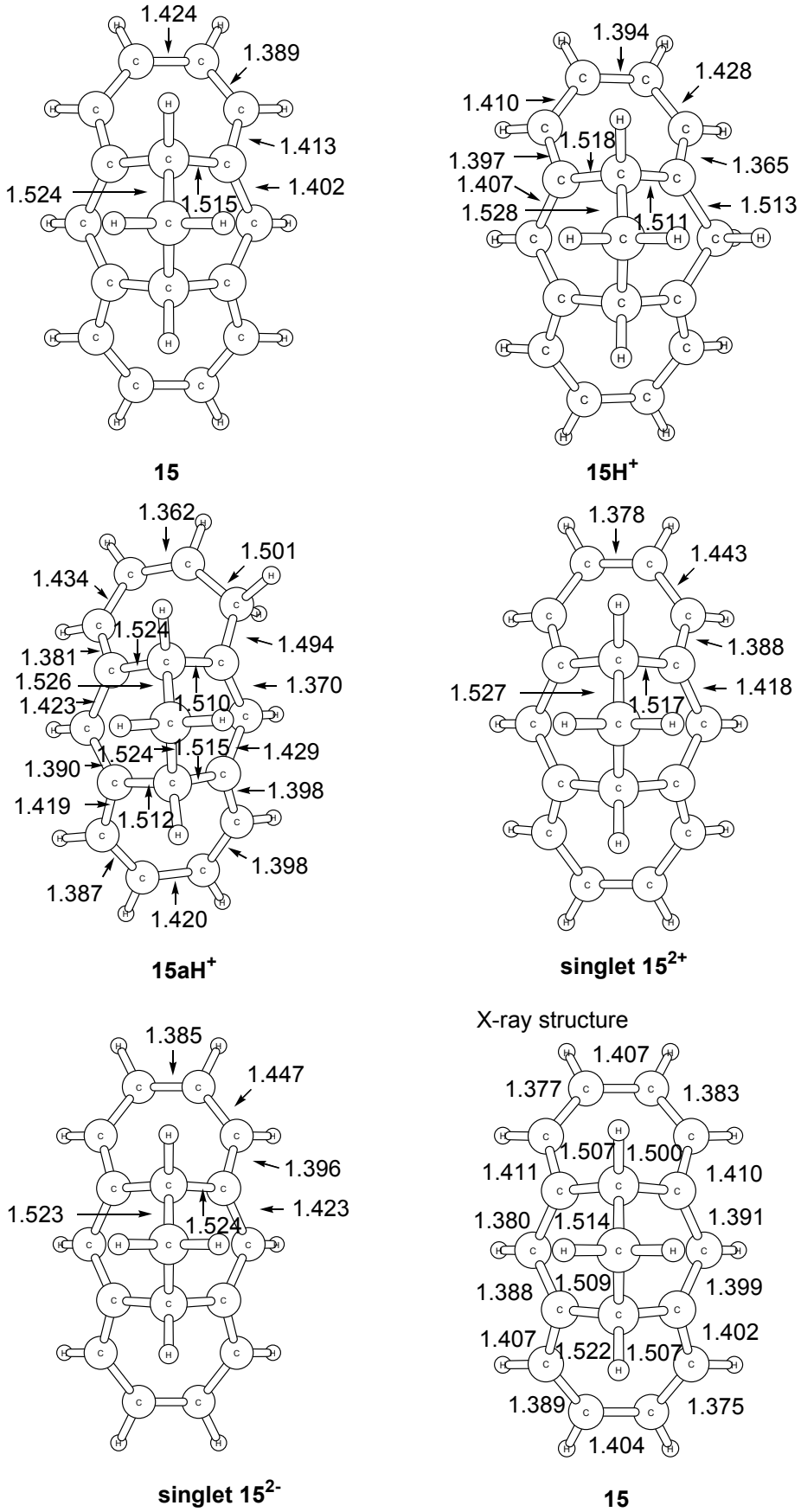

Fig S18. B3LYP/6-31G(d) optimized geometries for **15**, **15H**$^{+}$, **15aH**$^{+}$, singlet **15**$^{2+}$, and singlet **15**$^{2-}$ and X-ray structure for **15** (bond length, Å).

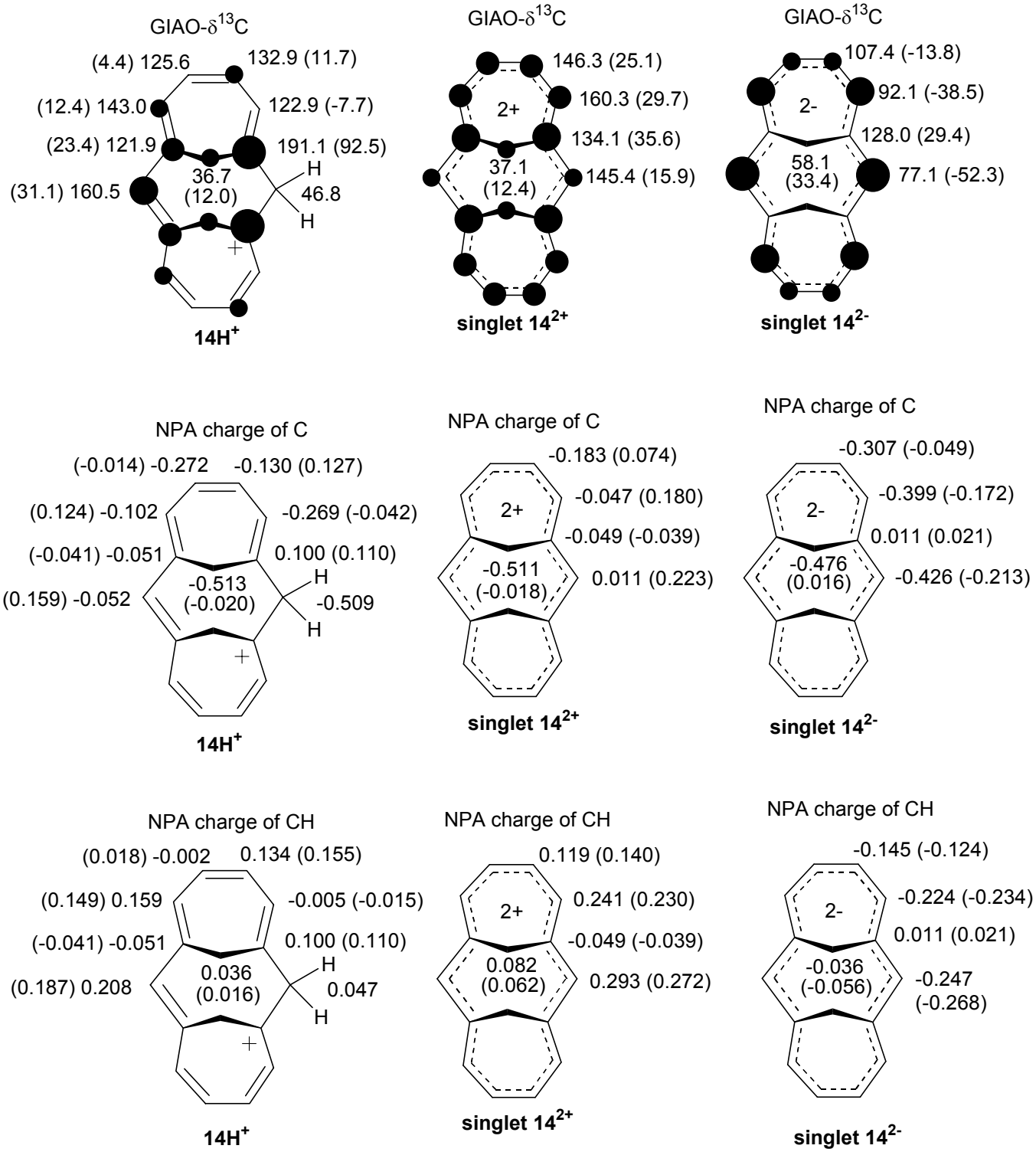

Fig S19. Computed ^{13}C NMR chemical shifts, NPA-derived carbon charges, and NPA-derived overall charges over CH units for **14H**$^{+}$, **14**$^{2+}$, and **14**$^{2-}$ at B3LYP/6-31G(d) level ($\Delta\delta$ ^{13}C's and Δcharges relative to **14** in parentheses). [*Dark circles are roughly proportional to the magnitude of* $\Delta\delta$ ^{13}*Cs (positive/downfield for the carbocations/dication and negative/upfield for the dianion); threshold was set to 10 ppm]*.

GIAO-δ^{13}C

B3LYP/6-311++G(3df,3pd)//B3LYP/6-31G(d)

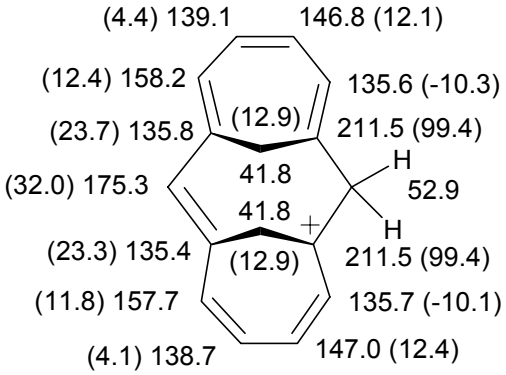

B3LYP/6-31+G(d,p)//B3LYP/6-31G(d)

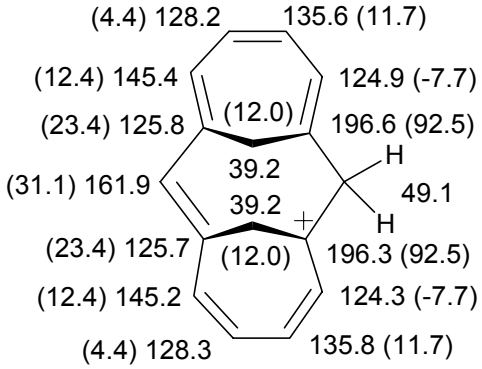

B3LYP/6-311++G(d,p)//B3LYP/6-31G(d)

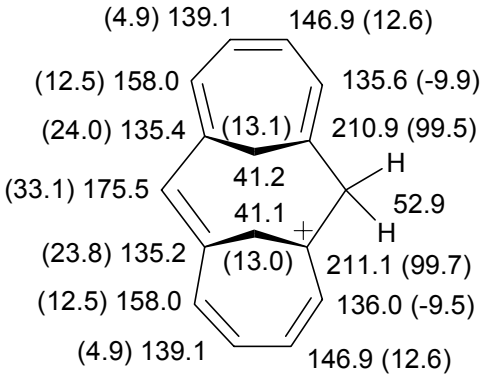

B3LYP/6-311++G(d,p)//B3LYP/6-311++G(d,p)

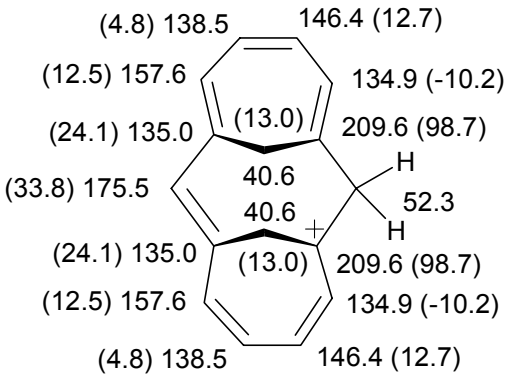

B3LYP/6-31G(d)//B3LYP/6-31G(d)

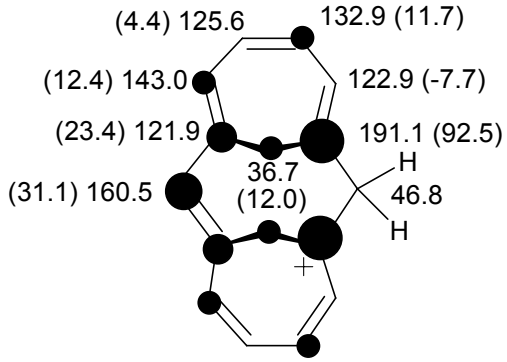

Experimental-δ^{13}C
(in superacid solution)

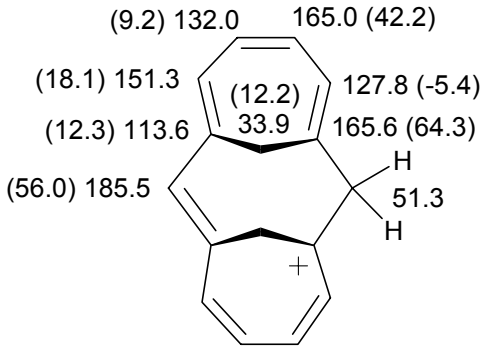

Fig S20. Experimental (Ref 22) and computed ^{13}C NMR chemical shifts for **14H**$^{+}$.

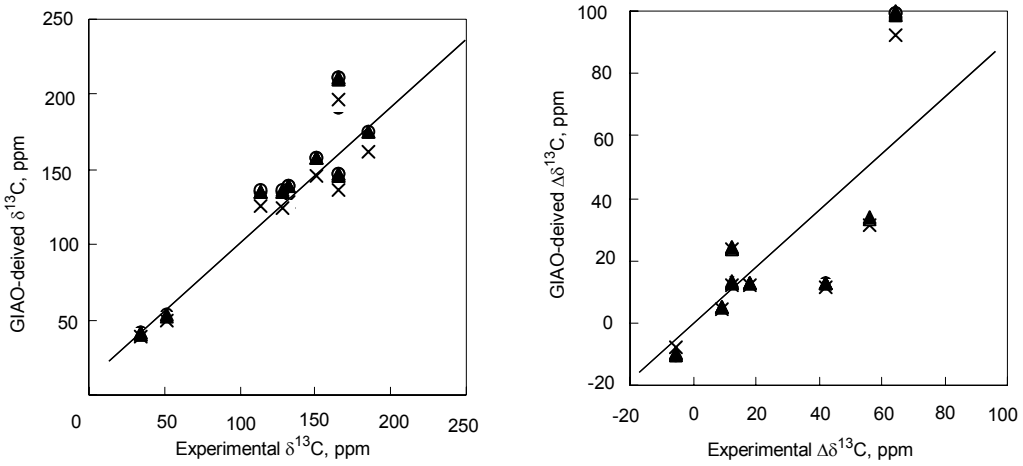

Figure S20a. Plots of experimental $\delta^{13}C$ vs GIAO-derived $\delta^{13}C$ and experimental $\Delta\delta^{13}C$ vs GIAO-derived $\Delta\delta^{13}C$ for **14H**$^{+}$ by (○) B3LYP/6-31G(d)//B3LYP/6-31G(d), (●) B3LYP/6-31+G(d,p)//B3LYP/6-31G(d), (×) B3LYP/6-311++G(d,p)//B3LYP/6-31G(d), (Δ) B3LYP/6-311++G(3df,3pd)//B3LYP/6-31G(d), (▲) B3LYP/6-311++G(d,p)//B3LYP/6-311++G(d,p).

GIAO-δ^{13}C

B3LYP/6-311++G(3df,3pd)//B3LYP/6-31G(d)

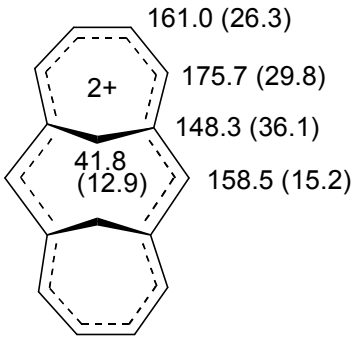

B3LYP/6-31+G(d,p)//B3LYP/6-31G(d)

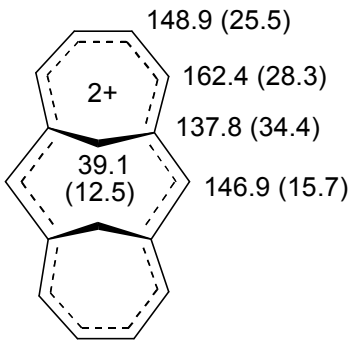

B3LYP/6-311++G(d,p)//B3LYP/6-31G(d)

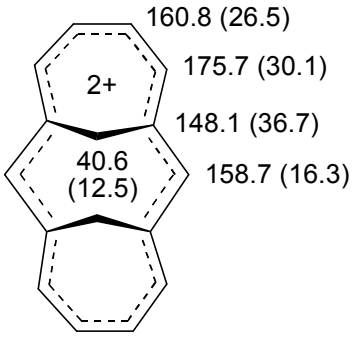

B3LYP/6-311++G(d,p)//B3LYP/6-311++G(d,p)

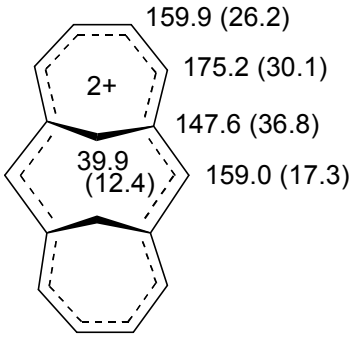

B3LYP/6-31G(d)//B3LYP/6-31G(d)

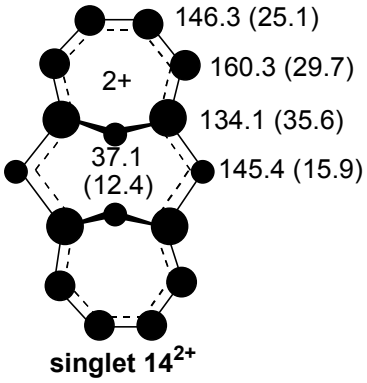

singlet 14^{2+}

Experimental-δ^{13}C
(in superacid solution)

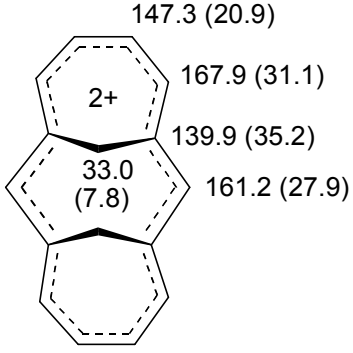

Fig S21. Experimental (Ref 22) and computed ^{13}C NMR chemical shifts for singlet $\mathbf{14}^{2+}$.

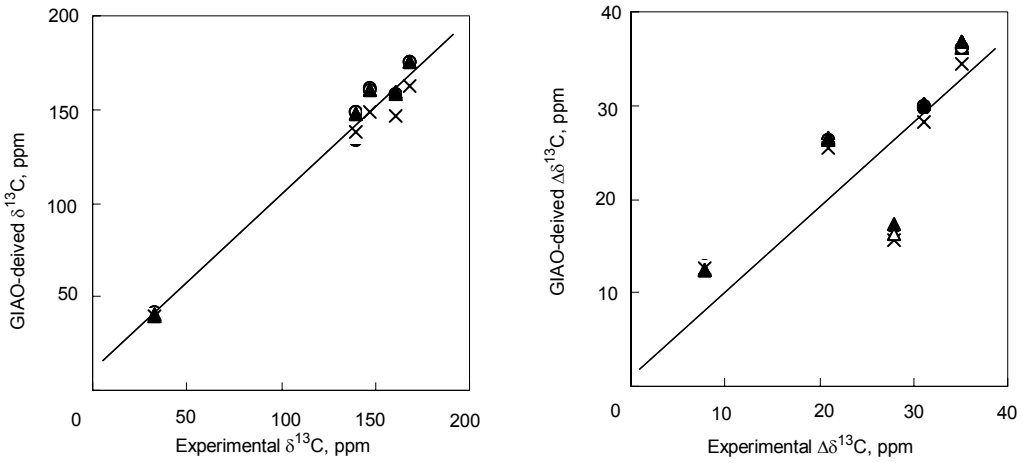

Figure S21a. Plots of experimental $\delta^{13}C$ vs GIAO-derived $\delta^{13}C$ and experimental $\Delta\delta^{13}C$ vs GIAO-derived $\Delta\delta^{13}C$ for **14**$^{2+}$ by (○) B3LYP/6-31G(d)//B3LYP/6-31G(d), (●) B3LYP/6-31+G(d,p)//B3LYP/6-31G(d), (×) B3LYP/6-311++G(d,p)//B3LYP/6-31G(d), (Δ) B3LYP/6-311++G(3df,3pd)//B3LYP/6-31G(d), (▲) B3LYP/6-311++(d,p)//B3LYP/6-311++G(d,p).

GIAO-δ^{13}C

B3LYP/6-311++G(3df,3pd)//B3LYP/6-31G(d)

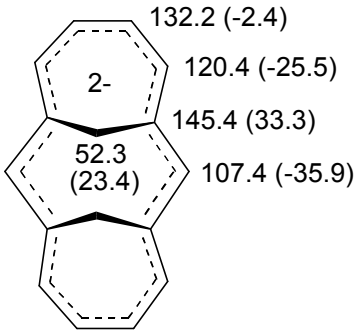

B3LYP/6-31+G(d,p)//B3LYP/6-31G(d)

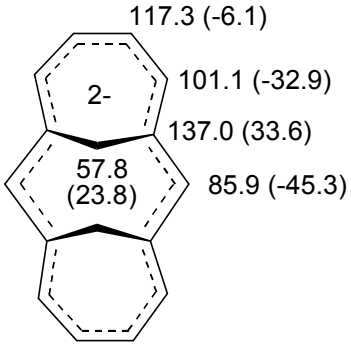

B3LYP/6-311++G(d,p)//B3LYP/6-31G(d)

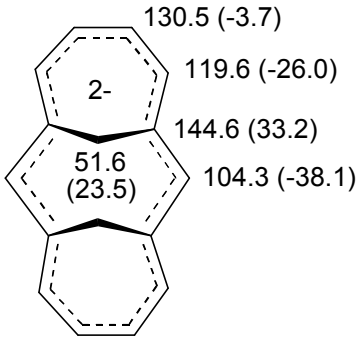

B3LYP/6-311++G(d,p)//B3LYP/6-311++G(d,p)

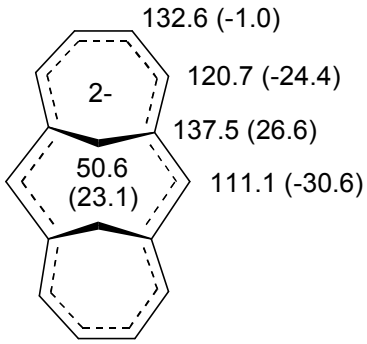

B3LYP/6-31G(d)//B3LYP/6-31G(d)

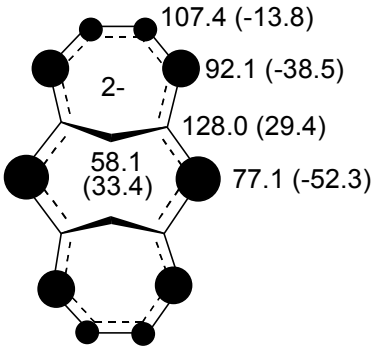

Experimental-δ^{13}C
(in THF-d_8)

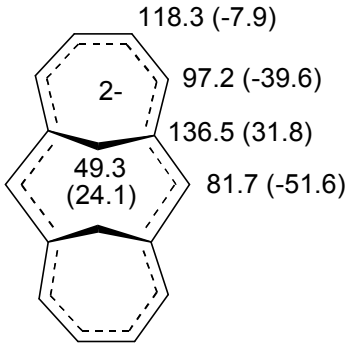

Fig S21b. Experimental (Ref 21) and computed ^{13}C NMR chemical shifts for singlet $\mathbf{14}^{2-}$.

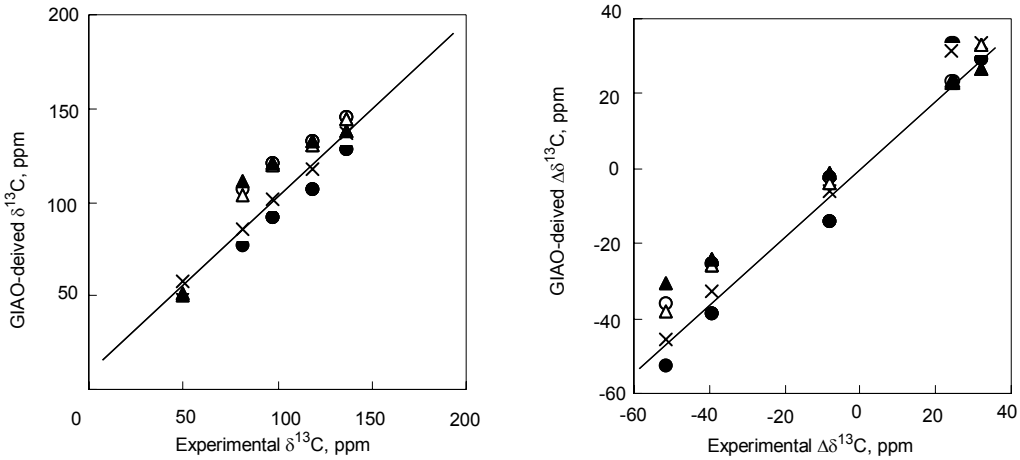

Figure S21c. Plots of experimental $\delta^{13}C$ vs GIAO-derived $\delta^{13}C$ and experimental $\Delta\delta^{13}C$ vs GIAO-derived $\Delta\delta^{13}C$ for **14**$^{2-}$ by (○) B3LYP/6-31G(d)//B3LYP/6-31G(d), (●) B3LYP/6-31+G(d,p)//B3LYP/6-31G(d), (×) B3LYP/6-311++G(d,p)//B3LYP/6-31G(d), (Δ) B3LYP/6-311++G(3df,3pd)//B3LYP/6-31G(d), (▲) B3LYP/6-311++G(d,p)//B3LYP/6-311++G(d,p).

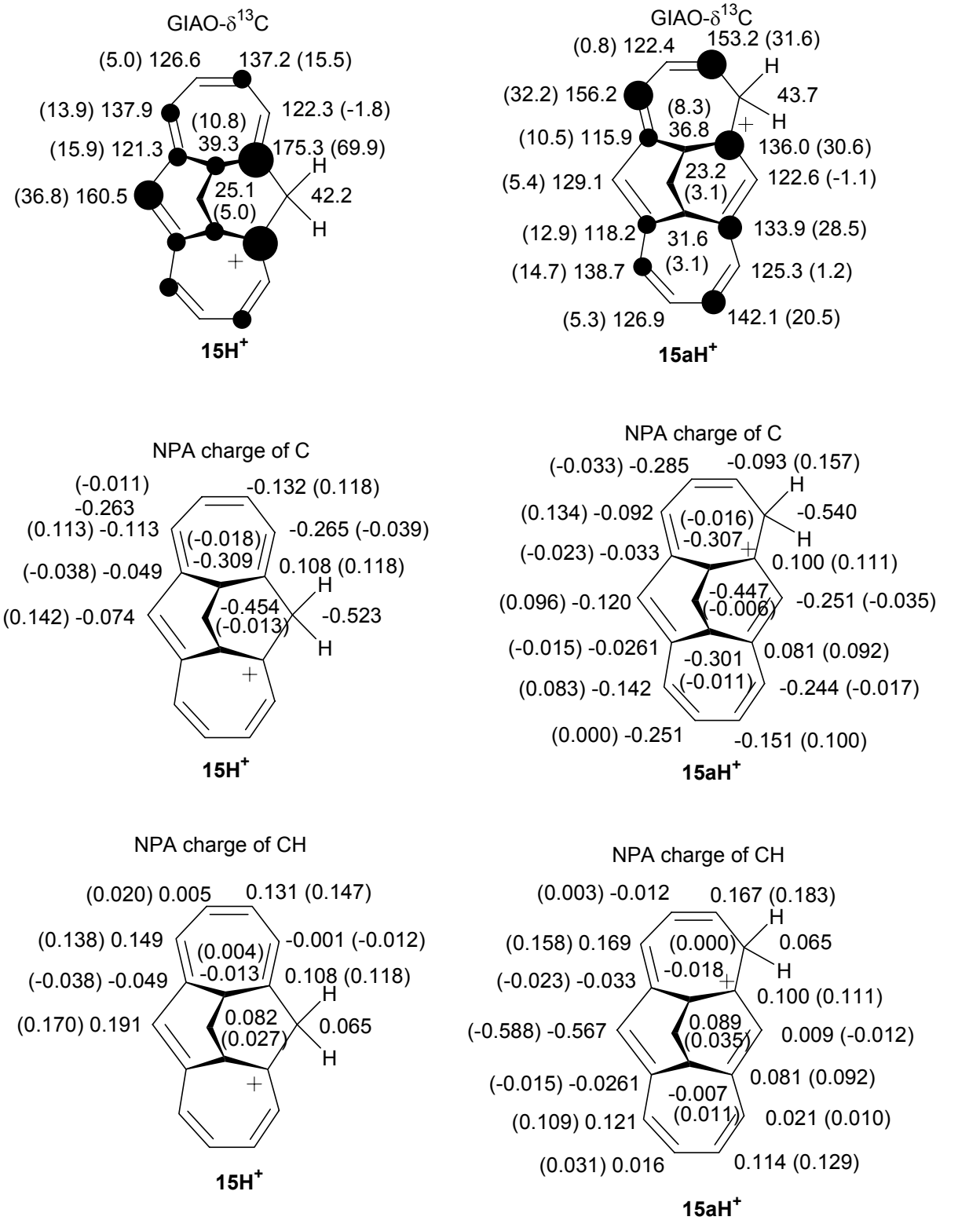

Fig S22. Computed ^{13}C NMR chemical shifts, NPA-derived carbon charges, and NPA-derived overall charges over CH units for **15H**$^{+}$, **15aH**$^{+}$, **15**$^{2+}$, and **15**$^{2-}$ at B3LYP/6-31G(d) level ($\Delta\delta$ ^{13}C's and Δcharges relative to **15** in parentheses). [*Dark circles are roughly proportional to the magnitude of $\Delta\delta^{13}$Cs (positive/downfield for the carbocations/dication and negative/upfield for the dianion); threshold was set to 10 ppm]*.

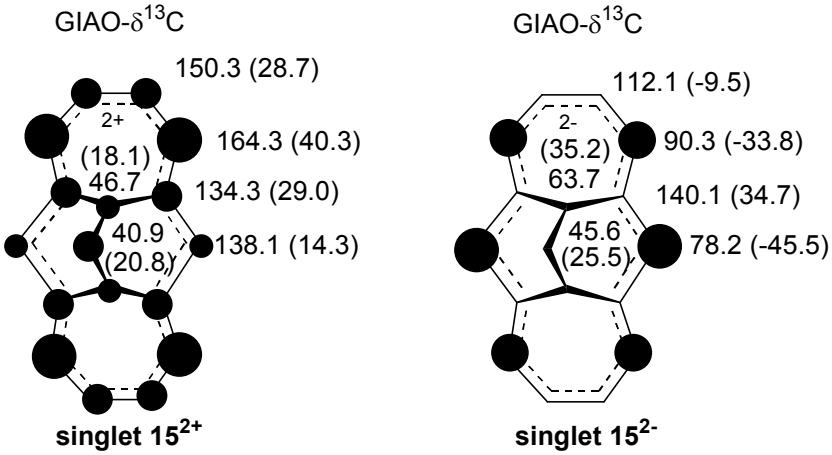

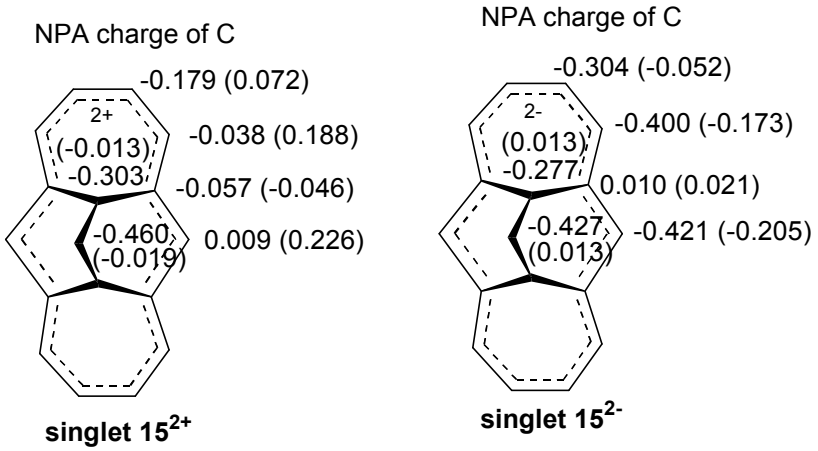

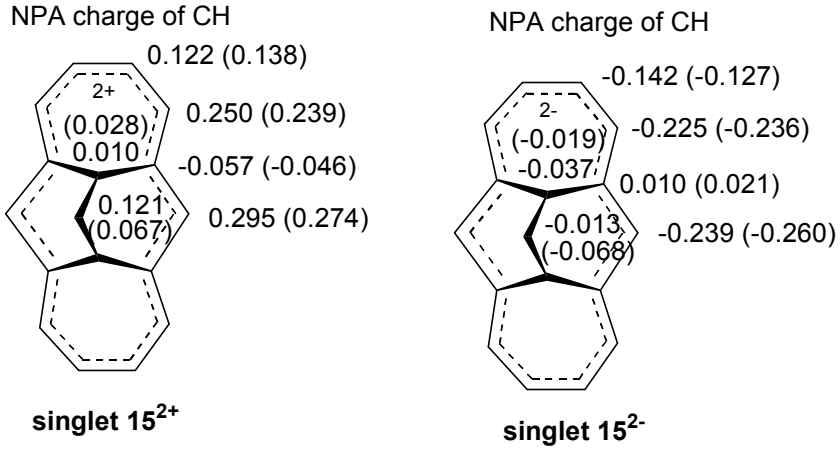

Fig S22 (continued).

GIAO-δ^{13}C

B3LYP/6-311++G(3df,3pd)//B3LYP/6-31G(d)

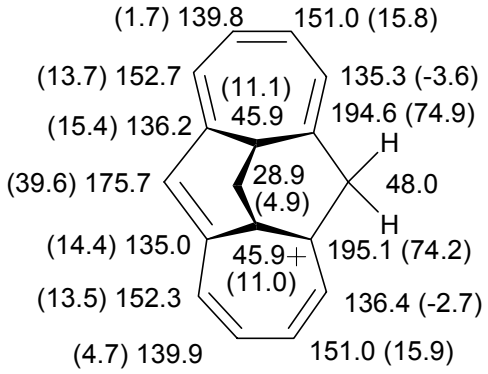

B3LYP/6-31+G(d,p)//B3LYP/6-31G(d)

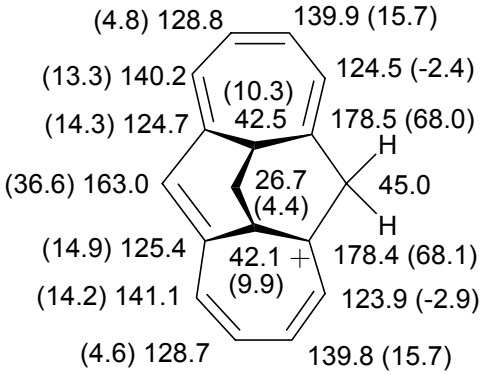

B3LYP/6-311++G(d,p)//B3LYP/6-31G(d)

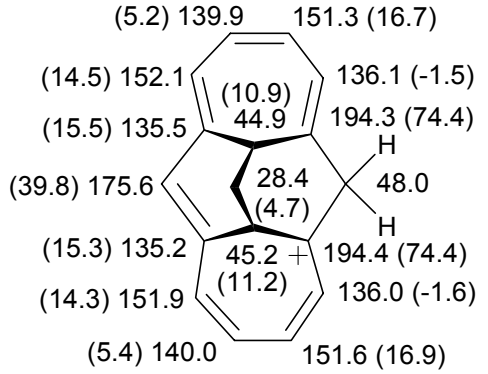

B3LYP/6-311++G(d,p)//B3LYP/6-311++G(d,p)

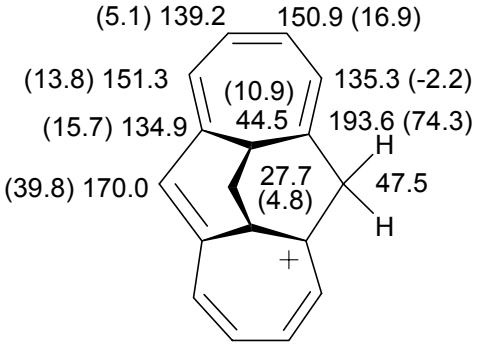

B3LYP/6-31G(d)//B3LYP/6-31G(d)

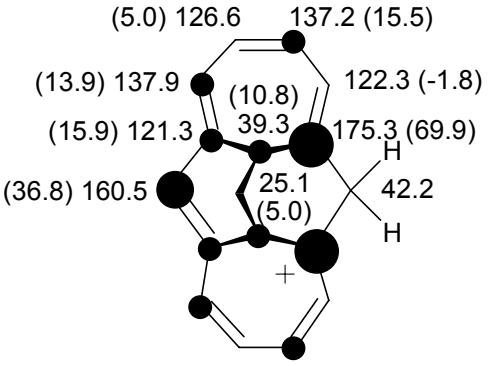

Experimental-δ^{13}C

(in superacid solution)

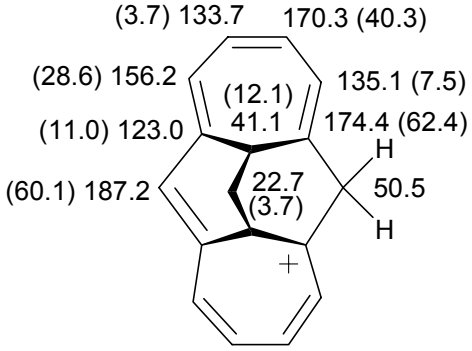

Fig S22a. Experimental (Ref 21) and computed ^{13}C NMR chemical shifts for **15H**$^{+}$.

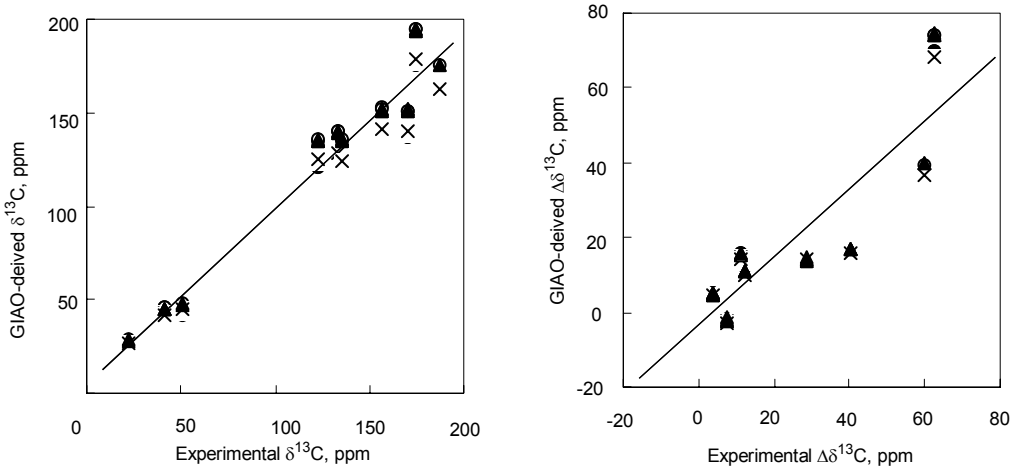

Figure S22b. Plots of experimental $\delta^{13}C$ vs GIAO-derived $\delta^{13}C$ and experimental $\Delta\delta^{13}C$ vs GIAO-derived $\Delta\delta^{13}C$ for **15H$^+$** by (○) B3LYP/6-31G(d)//B3LYP/6-31G(d), (●) B3LYP/6-31+G(d,p)//B3LYP/6-31G(d), (×) B3LYP/6-311++G(d,p)//B3LYP/6-31G(d), (Δ) B3LYP/6-311++G(3df,3pd)//B3LYP/6-31G(d), (▲) B3LYP/6-311++G(d,p)//B3LYP/6-311++G(d,p).

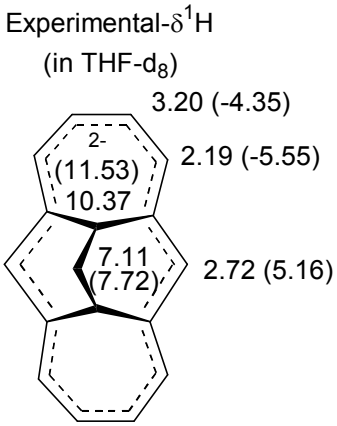

Fig S22c. Experimental ^1H NMR chemical shifts for singlet **15^{2-}** (Ref. 21).

GIAO-δ^{13}C

B3LYP/6-311++G(3df,3pd)//B3LYP/6-31G(d)

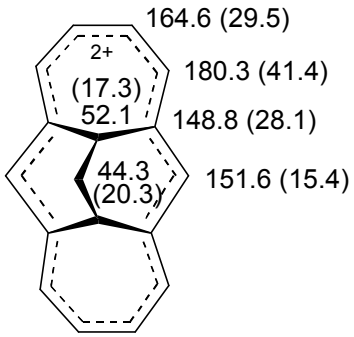

B3LYP/6-31+G(d,p)//B3LYP/6-31G(d)

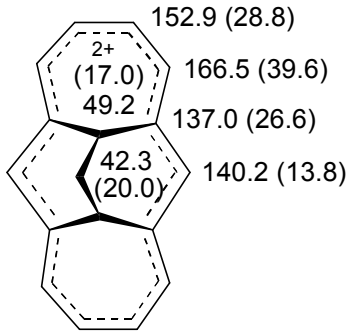

B3LYP/6-311++G(d,p)//B3LYP/6-31G(d)

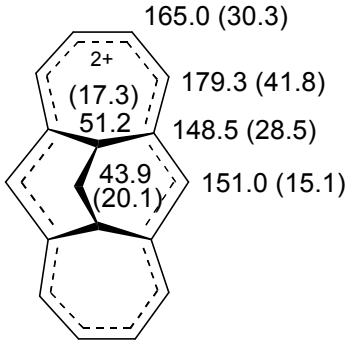

B3LYP/6-311++G(d,p)//B3LYP/6-311++G(d,p)

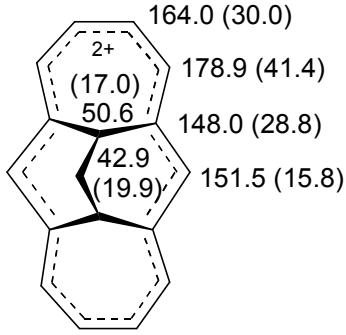

B3LYP/6-31G(d)//B3LYP/6-31G(d)

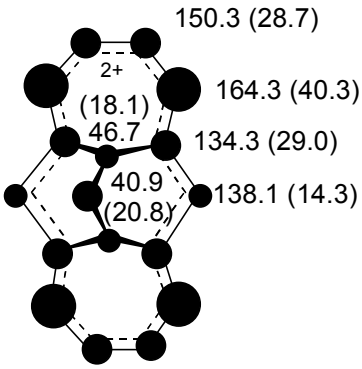

Experimental-δ^{13}C
(in superacid solution)

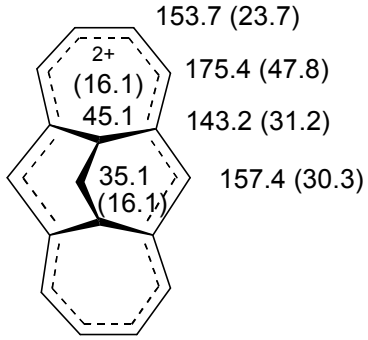

Fig S22d. Experimental (Ref 22) and computed ^{13}C NMR chemical shifts for singlet $\mathbf{15}^{2+}$.

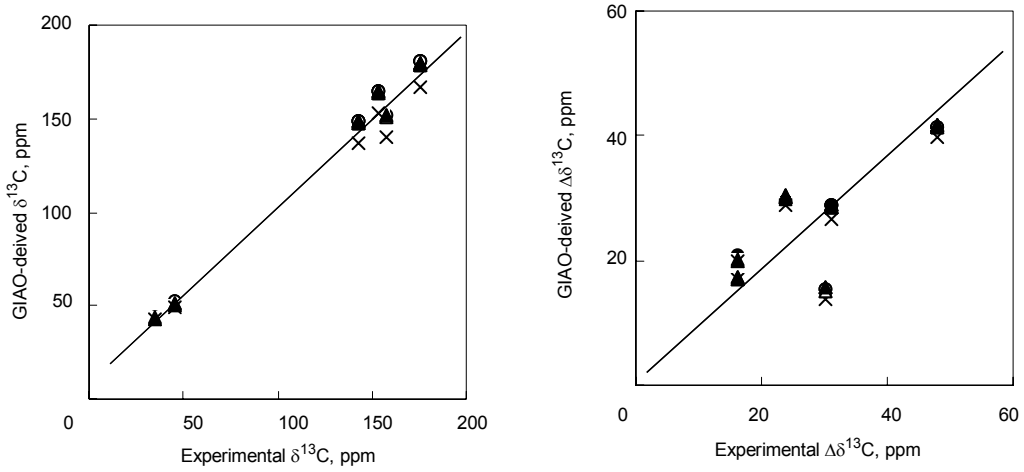

Figure S22e. Plots of experimental $\delta^{13}C$ vs GIAO-derived $\delta^{13}C$ and experimental $\Delta\delta^{13}C$ vs GIAO-derived $\Delta\delta^{13}C$ for $\mathbf{15}^{2+}$ by (○) B3LYP/6-31G(d)//B3LYP/6-31G(d), (●) B3LYP/6-31+G(d,p)//B3LYP/6-31G(d), (×) B3LYP/6-311++G(d,p)//B3LYP/6-31G(d), (Δ) B3LYP/6-311++G(3df,3pd)//B3LYP/6-31G(d), (▲) B3LYP/6-311++G(d,p)//B3LYP/6-311++G(d,p).

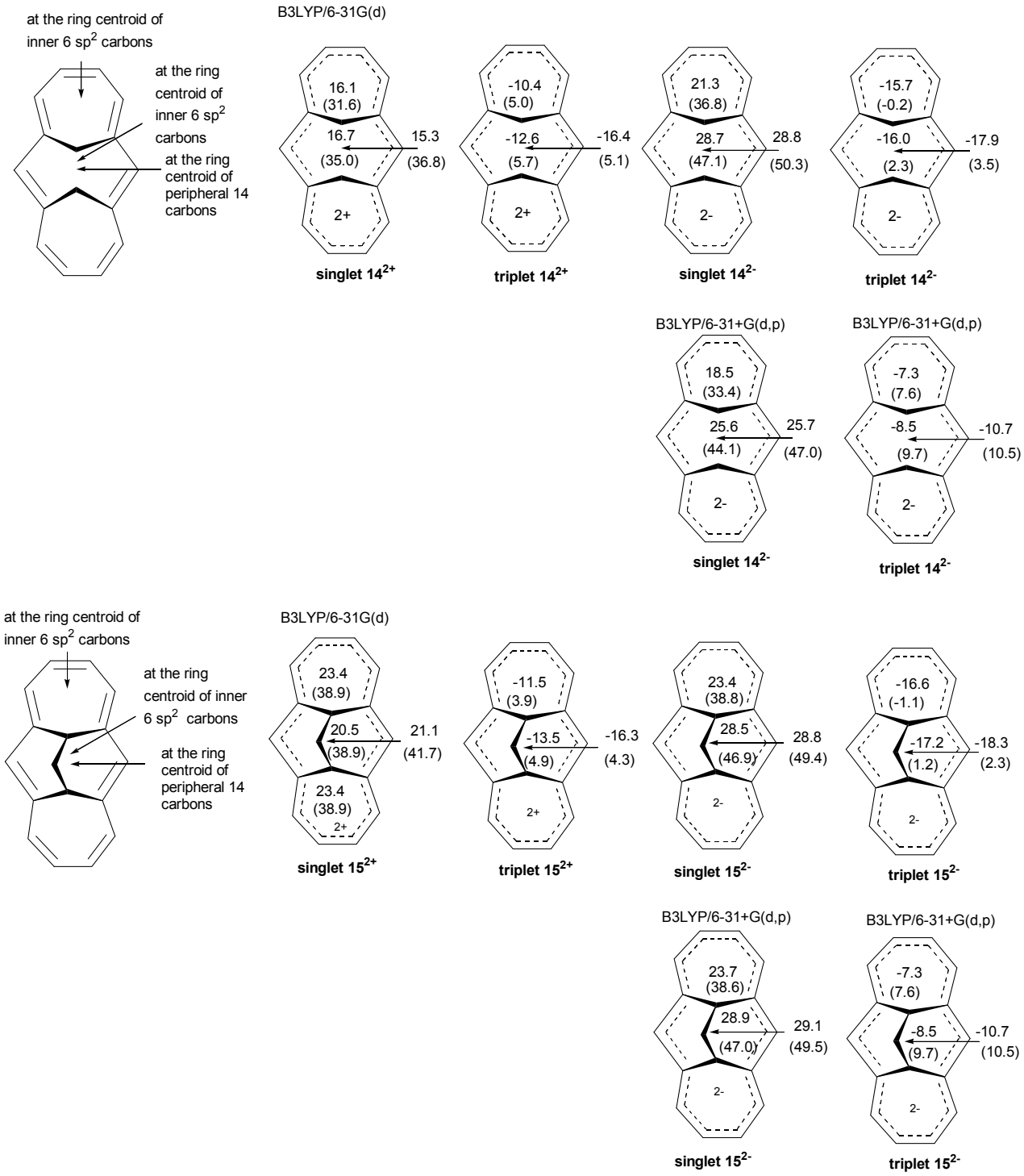

Fig S23. NICS values for $\mathbf{14}^{2+}$, $\mathbf{14}^{2-}$, $\mathbf{15}^{2+}$, and $\mathbf{15}^{2-}$ at B3LYP/6-31G(d) or 6-31+G(d,p) level (ΔNICS values relative to those of parent hydrocarbons **14** and **15** in parentheses).

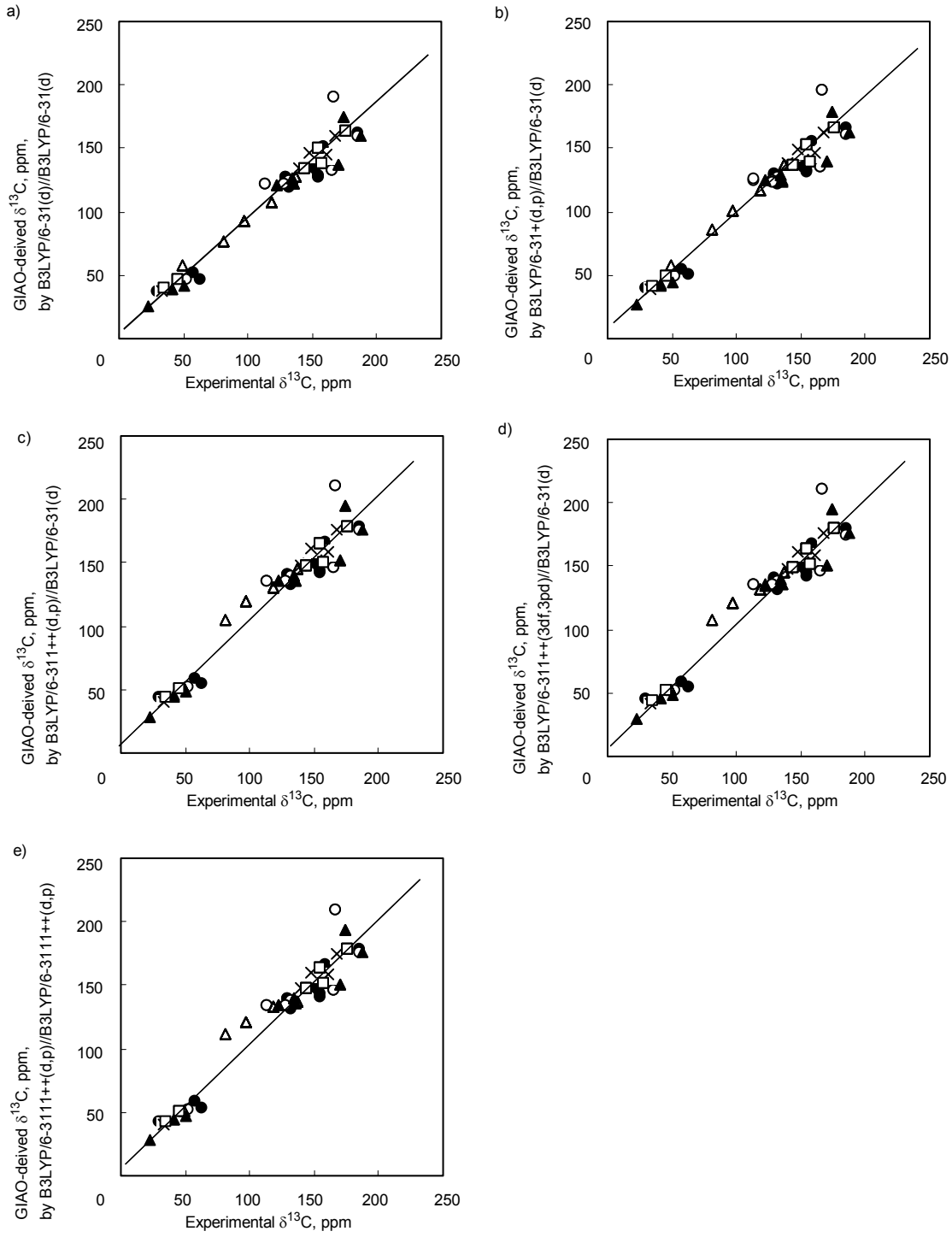

Fig S24. Plots of experimental $\delta^{13}C$ vs GIAO-derived $\delta^{13}C$ by (a) B3LYP/6-31G(d)//B3LYP/6-31G(d), (b) B3LYP/6-31+G(d,p)//B3LYP/6-31G(d), (c) B3LYP/6-311++G(d,p)//B3LYP/6-31G(d), (d) B3LYP/6-311++G(3df,3pd)//B3LYP/6-31G(d), (e) B3LYP/6-311++G(d,p)//B3LYP/6-311++G(d,p) (○: **10aH**$^+$, ●: **14H**$^+$, ×: singlet **14**$^{2+}$, Δ: singlet **14**$^{2-}$, ▲: **15H**$^+$, □: singlet **15**$^{2+}$).

Addendum to Fig. S24

Computed $\delta^{13}C$ values correlate with the experimental data by equations (1-5) (see below) with R^2 = 0.94-0.95 and a slope of 0.89-0.96. The slopes at higher basic sets are closer to unity, although correlation coefficients R^2 are similar.

B3LYP/6-31(d)//B3LYP/6-31(d):

$$\delta^{13}C\ (GIAO) = 0.89 \times \delta^{13}C\ (experimental) + 6.4 \qquad R^2 = 0.951 \qquad (1)$$

B3LYP/6-31+G(d,p)//B3LYP/6-31G(d):

$$\delta^{13}C\ (GIAO) = 0.89 \times \delta^{13}C\ (experimental) + 10.2 \qquad R^2 = 0.947 \qquad (2)$$

B3LYP/6-311++G(d,p)//B3LYP/6-31G(d):

$$\delta^{13}C\ (GIAO) = 0.96 \times \delta^{13}C\ (experimental) + 11.3 \qquad R^2 = 0.942 \qquad (3)$$

B3LYP/6-311++G(3df,3pd)//B3LYP/6-31G(d):

$$\delta^{13}C\ (GIAO) = 0.95 \times \delta^{13}C\ (experimental) + 12.3 \qquad R^2 = 0.940 \qquad (4)$$

B3LYP/6-311++G(d,p)//B3LYP/6-311++G(d,p):

$$\delta^{13}C\ (GIAO) = 0.96 \times \delta^{13}C\ (experimental) + 11.4 \qquad R^2 = 0.938 \qquad (5)$$

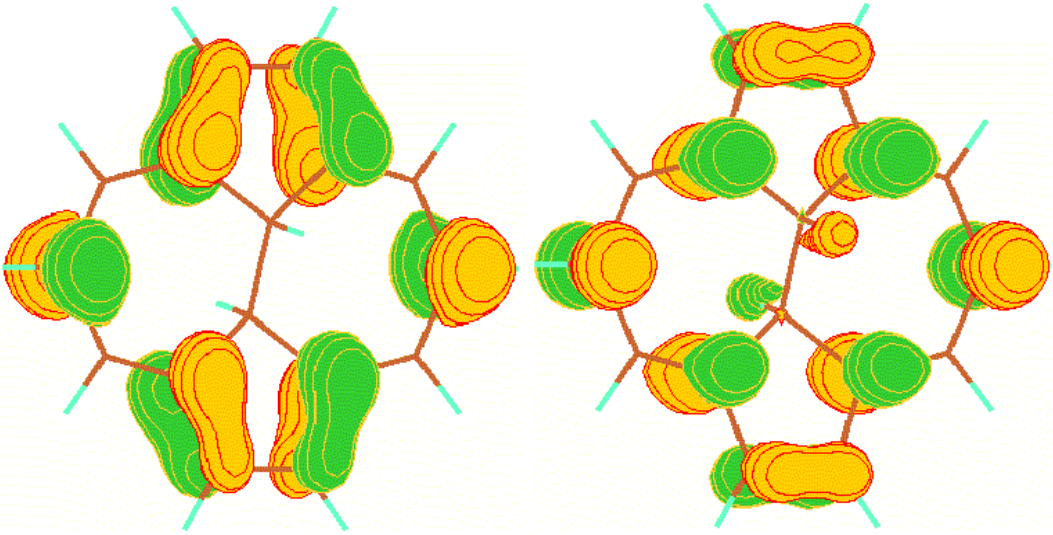

HOMO for **4** LUMO for **4**

Fig S25. Forms of HOMO, LUMO, and SOMO for **4**, **4bH**$^+$, triplet **4**$^{2+}$, and singlet **4**$^{2-}$ by B3LYP/6-31G(d).

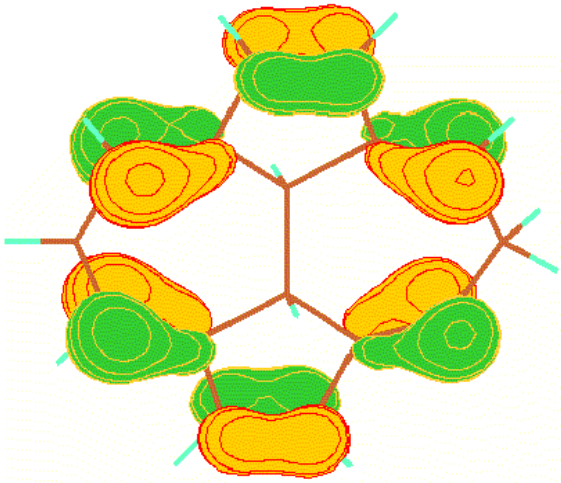

HOMO for **4bH**$^{+}$

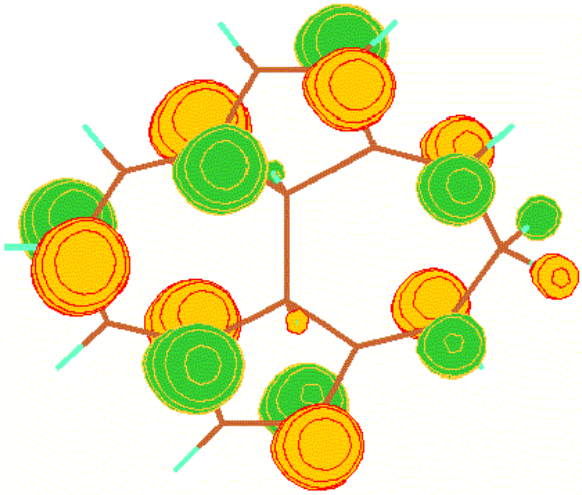

LUMO for **4bH**$^{+}$

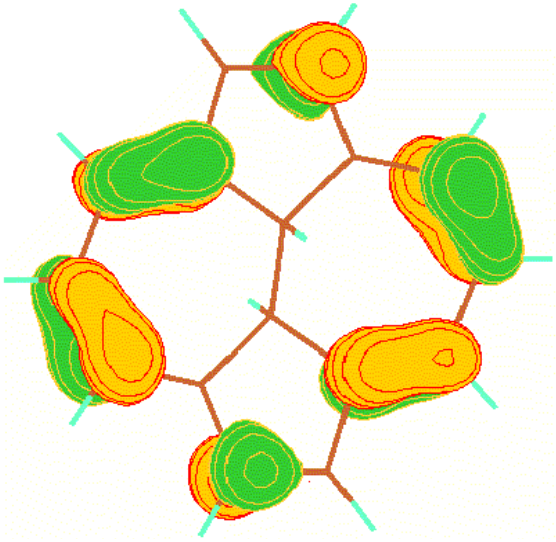

HOMO for singlet **4**$^{2+}$

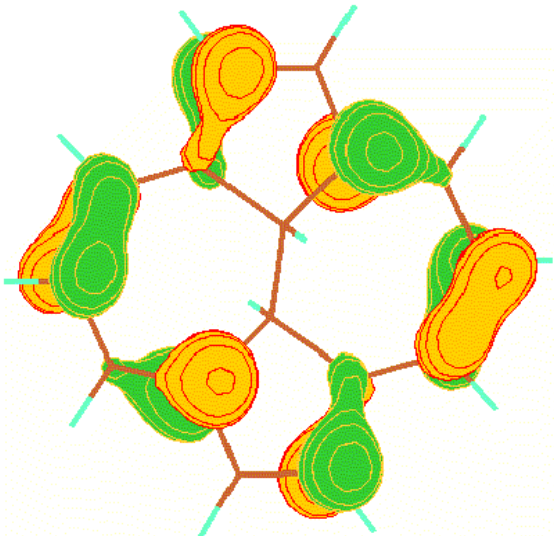

LUMO for singlet **4**$^{2+}$

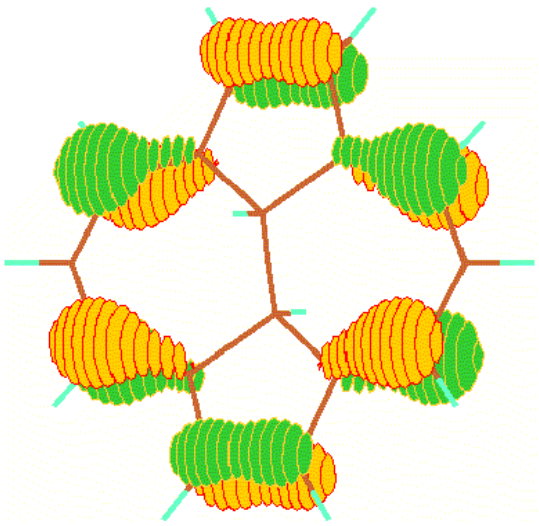

SOMO for triplet **4**$^{2+}$

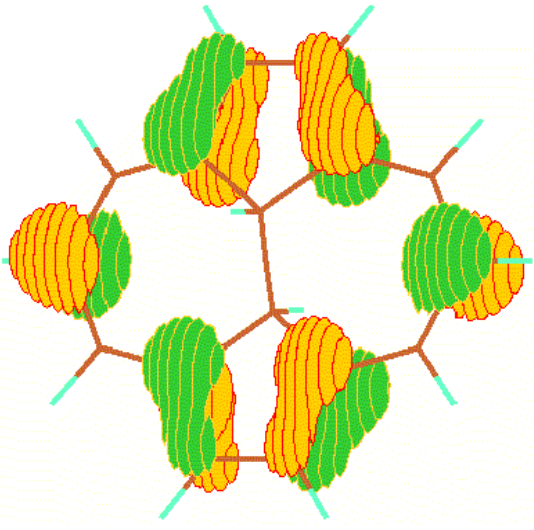

SOMO for triplet **4**$^{2+}$

Figure S25 (continued).

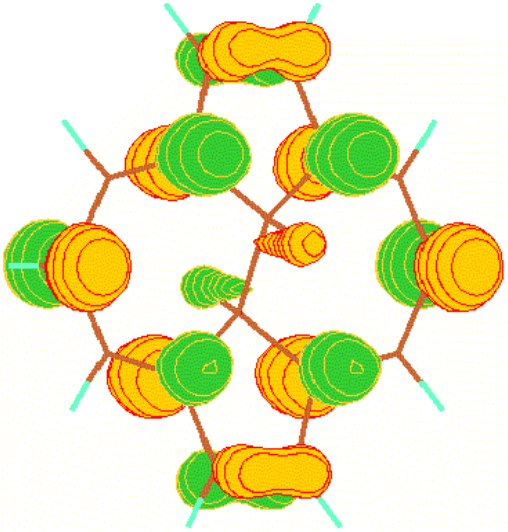

HOMO for singlet $\mathbf{4}^{2-}$

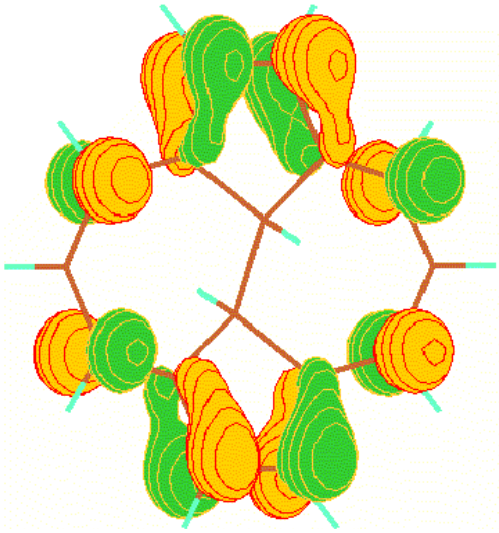

LUMO for singlet $\mathbf{4}^{2-}$

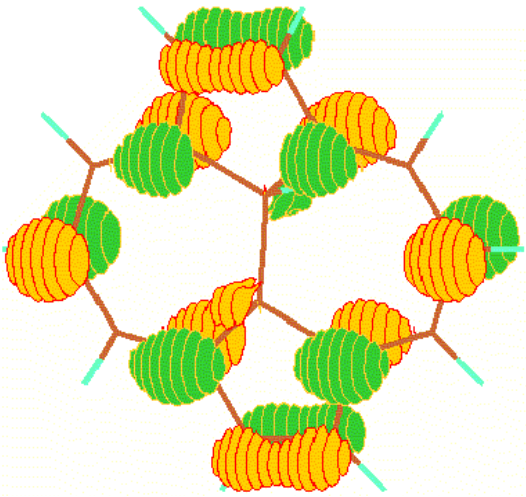

SOMO for triplet $\mathbf{4}^{2-}$

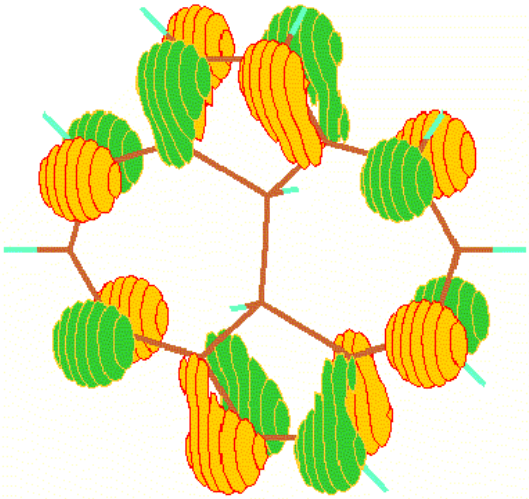

SOMO for triplet $\mathbf{4}^{2-}$

Figure S25 (continued).

Table S1. Energies (E), Zero Point Energies (ZPE), Gibbs Free Energies (G), and Relative Gibbs Free Energies (ΔG) for B3LYP/6-31G(d) Optimized Structures of Dihydro-derivatives **4**-**11**.

Compd	Molecular point group	E, hartree	ZPE, hartree	G, hartree	ΔG, kcal[a]
4	C_1	-616.8707181	0.228341	-616.678445	(0)
6	C_1	-616.8465659	0.228190	-616.654624	14.9
5	C_1	-695.4919074	0.284632	-695.245566	(0)
7	C_1	-695.4536401	0.284425	-695.207700	23.8
8	C_1	-616.8234724	0.228569	-616.630880	(0)
10	C_1	-616.8738954	0.228787	-616.681047	-31.5
9	C_1	-695.4358718	0.283847	-695.190422	(0)
11	C_1	-695.5004848	0.284624	-695.254083	-39.9

[a] Relative Gibbs free energies of *syn*-derivatives to those of *anti*-derivatives.

Table S2. Energies (E), Zero Point Energies (ZPE), Gibbs Free Energies (G), Relative Gibbs Free Energies (ΔG) for B3LYP/6-31G(d) Optimized Structures for **4**-**5**, **8**-**15**, their Monocations, Dications, and Dianions

Compd	Protonation site	Molecular point group	E, hartree[a]	ZPE, hartree[a]	G, hartree[a]	ΔG, kcal[b]
4		C_1	-616.8707181	0.228341	-616.678445	(0)
		C_{2h}	-616.8706817	0.228333	-616.677761	0.4
4H$^+$	C(1)	C_1	-617.2333368	0.240699	-617.029301	-220.2
4aH$^+$	C(3)	C_1	-617.234331	0.240751	-617.030422	-220.9
4bH$^+$	C(4)	C_1	-617.2384905	0.240730	-617.033830	-223.4
4^{2+} (s)[c]		C_1	-616.2230611	0.228640	-616.031314	406.1
		C_i	-616.2230366	0.228626	-616.031306	406.1
		C_{2h}[d]	-616.2214584	0.226870	-616.030650	406.5
4^{2+} (t)[c]		C_1	-616.2244602	0.228783	-616.033230	404.9
		C_s	-616.2244602	0.228777	-616.033237	
		C_{2h}	-616.2244166	0.228773	-616.032542	405.3
4^{2-} (s)[c]		C_1	-616.7220175	0.218179	-616.540687	86.4
		C_{2h}	-616.7219216	0.218157	-616.539974	86.9
4^{2-} (t)[c]		C_1	-616.7181169	0.217782	-616.538074	88.1
		C_{2h}	-616.7180712	0.217772	-616.537382	88.5
5		C_1	-695.4919074	0.284632	-695.245566	(0)
		C_{2h}	-695.4918974	0.284623	-695.244913	0.4
5H$^+$	C(1)	C_1	-695.8578678	0.296845	-695.599860	-222.3
5aH$^+$	C(3)	C_1	-695.8578801	0.296912	-695.600027	-222.4
5bH$^+$	C(4)	C_1	-695.8615373	0.297000	-695.603381	-224.5
5^{2+} (s)[c]		C_i	-694.8542078	0.284409	-694.608866	399.5
		C_{2h}[d]	-694.8534797	0.282958	-694.608601	399.7
		C_1	-694.8542025	0.284498	-694.608694	399.6
5^{2+} (t)[c]		C_{2h}	-694.8545546	0.284792	-694.608847	399.5
		C_1	-694.8545828	0.284811	-694.609502	399.1
5^{2-} (s)[c]		C_{2h}	-695.3532913	0.273662	-695.118077	80.0
		C_1	-695.3533188	0.273624	-695.118835	79.5
5^{2-} (t)[c]		C_{2h}	-695.3467395	0.273701	-695.112390	83.6
		C_1	-695.3467665	0.273722	-695.113043	83.2

[a] 1 hartree = 627.5096 kcal/mol. [b] Relative Gibbs free energies to those of the parent hydrocarbons. [c] (s) and (t) denote triplet and singlet states. [d] Number of imaginary frequencies = 1.

Table S2 (continued).

Compd	Protonation site	Molecular point group	E, hartree[a]	ZPE, hartree[a]	G, hartree[a]	ΔG, kcal[b]
8		C_{2h}	-616.8234939	0.228588	-616.630225	0.4
		C_1	-616.8234724	0.228569	-616.630880	(0)
8H$^+$	C(5)	C_1	-617.1897954	0.240435	-616.986002	-222.8
8aH$^+$	C(1)	C_1	-617.1836447	0.240668	-616.979726	-218.9
8bH$^+$	C(2)	C_1	-617.1886921	0.240909	-616.984366	-221.8
8^{2+} (s)[c]		C_{2h}	-616.1844352	0.229021	-615.991327	401.3
		C_1	-616.1844054	0.228991	-615.991986	400.9
8^{2+} (t)[c]		C_{2h}	-616.1731913	0.228392	-615.981566	407.5
		C_1	-616.1731519	0.228345	-615.982242	407.0
8^{2-} (s)[c]		C_{2h}	-616.7091687	0.218790	-616.526239	65.7
		C_1	-616.7091512	0.218781	-616.526889	65.3
8^{2-} (t)[c]		C_{2h}	-616.6988577	0.218887	-616.516534	71.8
		C_1	-616.6988251	0.218860	-616.517189	71.3
9		C_{2h}	-695.4358090	0.283771	-695.189819	0.4
		C_1	-695.4358718	0.283847	-695.190422	(0)
9H$^+$	C(5)	C_1	-695.8115965	0.296398	-695.554000	-228.1
9aH$^+$	C(1)	C_1	-695.7989077	0.295817	-695.542439	-220.9
9bH$^+$	C(2)	C_1	-695.8035653	0.295982	-695.546766	-223.6
9^{2+} (s)[c]		C_{2h}	-694.8082124	0.284235	-694.562690	393.9
		C_1	-694.8081658	0.284146	-694.563478	393.4
9^{2+} (t)[c]		C_{2h}	-694.7976001	0.283432	-694.553371	399.8
		C_1	-694.7975569	0.283357	-694.554107	399.3
9^{2-} (s)[c]		C_{2h}[b]	-695.3236722	0.273068	-695.088935	63.7
		C_1	-695.3238175	0.273755	-695.089723	63.2
9^{2-} (t)[c]		C_{2h}	-695.3166255	0.274226	-695.081418	68.4
		C_1	-695.3166141	0.274213	-695.082080	68.0

Table S2 (continued).

Compd	Protonation site	Molecular point group	E, hartree[a]	ZPE, hartree[a]	G, hartree[a]	ΔG, kcal[b]
10		C_{2v}	-616.8738954	0.228787	-616.680393	0.4
		C_1	-616.8738954	0.228787	-616.681047	(0)
10H$^+$	C(5)	C_s	-617.2300612	0.240586	-617.025966	-216.4
		C_1	-617.2300612	0.240586	-617.025967	-216.4
10aH$^+$	C(1)	C_1	-617.2391727	0.240969	-617.034712	-221.9
10bH$^+$	C(2)	C_1	-617.235936	0.240777	-617.031813	-220.1
10^{2+} (s)[c]		C_{2v}	-616.2188396	0.228383	-616.026611	410.6
		C_1	-616.2188396	0.228383	-616.027265	410.3
10^{2+} (t)[c]		C_{2v}	-616.2169067	0.228321	-616.025267	411.5
		C_1	-616.2169067	0.228321	-616.025921	411.1
10^{2-} (s)[c]		C_s	-616.7470000	0.218961	-616.564409	73.2
		C_1	-616.7469915	0.218991	-616.564379	73.2
10^{2-} (t)[c]		C_s	-616.7283051	0.218584	-616.547035	84.1
		C_1	-616.7282851	0.218561	-616.547050	84.1
11		C_{2v}	-695.5004848	0.284624	-695.253430	0.4
		C_1	-695.5004848	0.284624	-695.254083	(0)
11H$^+$	C(5)	C_s	-695.8573173	0.296495	-695.599584	-216.8
		C_1	695.8573173	0.296495	-695.599584	-216.8
11aH$^+$	C(1)	C_1	-695.8675051	0.297025	-695.609250	-222.9
11bH$^+$	C(2)	C_1	-695.8636513	0.296574	-695.606023	-220.8
11^{2+} (s)[c]		C_{2v}	-694.8508447	0.284850	-694.604621	407.5
		C_1	-694.8508447	0.284850	-694.605275	407.1
11^{2+} (t)[c]		C_{2v}	-694.8487787	0.284259	-694.603589	408.2
		C_1	-694.8487787	0.284260	-694.604243	407.8
11^{2-} (s)[c]		C_{2v}	-695.3740715	0.274706	-695.137263	73.3
		C_1	-695.3740715	0.274707	-695.137917	72.9
11^{2-} (t)[c]		C_{2v}	-695.355764	0.274343	-695.120310	83.9
		C_1	-695.355764	0.274344	-695.120963	83.5

Table S2 (continued).

Compd	Protonation site	Molecular point group	E, hartree[a]	ZPE, hartree[a]	G, hartree[a]	ΔG, kcal[b]
14		C_{2v}	-618.0403323	0.252018	-617.823929	0.4
		C_1	-618.0403323	0.252019	-617.824583	(0)
14H$^+$	C(5)	C_s	-618.413039	0.264786	-618.184928	-226.1
		C_1	-618.413039	0.264786	-618.184928	-226.1
14aH$^+$	C(1)	C_1	-618.4120941	0.264625	-618.184096	-225.6
14^{2+} (s)[c]		C_{2v}	-617.3963755	0.252767	-617.179355	404.9
		C_1	-617.3963755	0.252767	-617.180009	404.5
14^{2+} (t)[c]		C_{2v}	-617.379102	0.251302	-617.164858	414.0
		C_1	-617.379102	0.251302	-617.165512	413.6
14^{2-} (s)[c]		C_{2v}	-617.904338	0.242016	-617.698569	79.1
		C_1	-617.904338	0.242016	-617.699222	78.7
14^{2-} (t)[c]		C_{2v}	-617.8882346	0.241606	-617.683725	88.4
		C_1	-617.8882346	0.241607	-617.684378	88.0
15		C_{2v}	-656.1807873	0.258796	-655.957611	0.4
		C_1	-656.1807873	0.258797	-655.958264	(0)
15H$^+$	C(5)	C_s	-656.5443439	0.271000	-656.310041	-220.7
		C_1	-656.5443439	0.271001	-656.310041	-220.7
15aH$^+$	C(1)	C_1	-656.5503302	0.271170	-656.315906	-224.4
15^{2+} (s)[c]		C_{2v}	-655.5347736	0.259031	-655.311582	405.8
		C_1	-655.5347736	0.259031	-655.312236	405.4
15^{2+} (t)[c]		C_{2v}	-655.5213722	0.258087	-655.300391	412.8
		C_1	-655.5213722	0.258088	-655.301044	412.4
15^{2-} (s)[c]		C_{2v}	-656.0498283	0.248739	-655.837188	76.0
		C_1	-656.0498283	0.248740	-655.837842	75.6
15^{2-} (t)[c]		C_{2v}	-656.0312338	0.248407	-655.819851	86.9
		C_1	-656.0312338	0.248408	-655.820504	86.4

Table S3. Energies (E), Zero Point Energies (ZPE), Gibbs Free Energies (G), Relative Gibbs Free Energies (ΔG) for Optimized Structures for **4**, its Monocations, Dications, and Dianions

Compd Protonation site basic set	Molecular point group	E, hartree	ZPE, hartree	G, hartree	ΔG, kcal[a]
4					
B3LYP/6-31G(d)	C_1	-616.8707181	0.228341	-616.678445	(0)
B3LYP/6-31+G(d,p)	C_1	-616.9102648	0.227337	-616.719035	(0)
B3LYP/6-31++G(d,p)	C_1	-616.910426	0.227363	-616.719166	(0)
4H$^+$ C(1)					
B3LYP/6-31G(d)	C_1	-617.2333368	0.240699	-617.029301	-220.2
B3LYP/6-31+G(d,p)	C_1	-617.2653618	0.239618	-617.062429	-215.5
B3LYP/6-31++G(d,p)	C_1	-617.2655807	0.239627	-617.062637	-215.5
4aH$^+$ C(3)					
B3LYP/6-31G(d)	C_1	-617.234331	0.240751	-617.030422	-220.9
B3LYP/6-31+G(d,p)	C_1	-617.266431	0.239662	-617.063632	-216.2
B3LYP/6-31++G(d,p)	C_1	-617.2667051	0.239676	-617.063890	-216.3
4bH$^+$ C(4)					
B3LYP/6-31G(d)	C_1	-617.2384905	0.240730	-617.033830	-223.4
B3LYP/6-31+G(d,p)	C_2	-617.2705073	0.239629	-617.066981	-218.3
B3LYP/6-31++G(d,p)	C_2	-617.2707331	0.239645	-617.067190	-218.4
4^{2+} (s)					
B3LYP/6-31G(d)	C_1	-616.2230611	0.228640	-616.031314	406.1
B3LYP/6-31+G(d,p)	C_1	-616.2489933	0.227759	-616.058145	414.7
B3LYP/6-31++G(d,p)	C_1	-616.2492048	0.227777	-616.058331	414.7
4^{2+} (t)					
B3LYP/6-31G(d)	C_1	-616.2244602	0.228783	-616.033230	404.9
B3LYP/6-31+G(d,p)	C_s	-616.2502732	0.227906	-616.059936	413.6
B3LYP/6-31++G(d,p)	C_s	-616.2505412	0.227939	-616.060160	413.5
4^{2-} (s)					
B3LYP/6-31G(d)	C_1	-616.7220175	0.218179	-616.540687	86.4
B3LYP/6-31+G(d,p)	C_i	-616.81053	0.218047	-616.629518	56.2
B3LYP/6-31++G(d,p)	C_i	-616.8154522	0.220108	-616.632721	54.2
4^{2-} (t)					
B3LYP/6-31G(d)	C_1	-616.7181169	0.217782	-616.538074	88.1
B3LYP/6-31+G(d,p)	C_1	-616.8027096	0.216199	-616.625230	58.9
B3LYP/6-31++G(d,p)	C_1	-616.8257125	0.221942[b]	-616.640690	49.0

[a] Relative energies to the neutral. [b] Number of imaginary frequency is 1.

Table S4. Energies for Optimized Structures for **5**, **8**, **9**, **10**, **11**, **14**, **15**, and their dianions by B3LYP/6-31+G(d,p)

Compd baisc set	Molecular point group	E, hartree	ZPE, hartree	G, hartree	ΔG, kcal[a]
5					
B3LYP/6-31G(d)	C_1	-695.4919074	0.284632	-695.245566	(0)
B3LYP/6-31+G(d,p)	C_1	-695.5373455	0.283160	-695.292516	(0)
$\mathbf{5}^{2-}$(s)					
B3LYP/6-31G(d)	C_1	-695.3533188	0.273624	-695.118835	79.5
B3LYP/6-31+G(d,p)	C_1	-695.4453828	0.273100	-695.211455	50.9
$\mathbf{5}^{2-}$(t)					
B3LYP/6-31G(d)	C_1	-695.3467665	0.273722	-695.113043	83.2
B3LYP/6-31+G(d,p)	C_1	-695.4356826	0.272290	-695.203664	55.8
8					
B3LYP/6-31G(d)	C_1	-616.8234724	0.228569	-616.630880	(0)
B3LYP/6-31+G(d,p)	C_1	-616.8639904	0.227603	-616.672389	(0)
$\mathbf{8}^{2-}$(s)					
B3LYP/6-31G(d)	C_1	-616.7091512	0.218781	-616.526889	65.3
B3LYP/6-31+G(d,p)	C_1	-616.7911433	0.216601	-616.612105	37.8
$\mathbf{8}^{2-}$(t)					
B3LYP/6-31G(d)	C_1	-616.6988251	0.218860	-616.517189	71.3
B3LYP/6-31+G(d,p)	C_1	-616.783247	0.217881	-616.602835	43.6
9					
B3LYP/6-31G(d)	C_1	-695.4358718	0.283847	-695.190422	(0)
B3LYP/6-31+G(d,p)	C_1	-695.4821086	0.282391	-695.238197	(0)
$\mathbf{9}^{2-}$(s)					
B3LYP/6-31G(d)	C_1	-695.3238175	0.273755	-695.089723	63.2
B3LYP/6-31+G(d,p)	C_1	-695.4115526	0.272225	-695.178851	37.2
$\mathbf{9}^{2-}$(t)					
B3LYP/6-31G(d)	C_1	-695.3166141	0.274213	-695.082080	68.0
B3LYP/6-31+G(d,p)	C_1	-695.4057966	0.272888	-695.172796	41.0

[b] Relative Gibbs free energies to those of the parent hydrocarbons. [b] Number of imaginary frequencies = 1.

Table S4 (continued).

Compd baisc set	Molecular point group	E, hartree	ZPE, hartree	G, hartree	ΔG, kcal[a]
10					
B3LYP/6-31G(d)	C_1	-616.8738954	0.228787	-616.681047	(0)
B3LYP/6-31+G(d,p)	C_1	-616.913608	0.227808	-616.721778	(0)
10^{2-}(s)					
B3LYP/6-31G(d)	C_s	-616.7470000	0.218961	-616.564409	73.2
B3LYP/6-31+G(d,p)	C_1	-616.8305483	0.217839	-616.649253	45.5
10^{2-}(t)					
B3LYP/6-31G(d)	C_1	-616.7282851	0.218561	-616.547050	84.1
B3LYP/6-31+G(d,p)	C_1	-616.8136409	0.217338	-616.634063	55.0
11					
B3LYP/6-31G(d)	C_1	-695.5004848	0.284624	-695.254083	(0)
B3LYP/6-31+G(d,p)	C_1	-695.5468117	0.283283	-695.301795	(0)
11^{2-}(s)					
B3LYP/6-31G(d)	C_1	-695.3740715	0.274707	-695.137917	72.9
B3LYP/6-31+G(d,p)	C_1	-695.4634247	0.273319	-695.228806	45.8
11^{2-}(t)					
B3LYP/6-31G(d)	C_1	-695.355764	0.274344	-695.120963	83.5
B3LYP/6-31+G(d,p)	C_1	-695.4472602	0.272326[b]	-695.214100	55.0
14					
B3LYP/6-31G(d)	C_1	-618.0403323	0.252019	-617.824583	(0)
B3LYP/6-31+G(d,p)	C_1	-618.0831353	0.250841	-617.868622	(0)
14^{2-}(s)					
B3LYP/6-31G(d)	C_1	-617.904338	0.242016	-617.699222	78.7
B3LYP/6-31+G(d,p)	C_1	-617.9946934	0.240771	-617.791012	48.7
14^{2-}(t)					
B3LYP/6-31G(d)	C_1	-617.8882346	0.241607	-617.684378	88.0
B3LYP/6-31+G(d,p)	C_1	-617.9804216	0.240607	-617.777831	57.0

Table S4 (continued).

Compd baisc set	Molecular point group	E, hartree	ZPE, hartree	G, hartree	ΔG, kcal[a]
15					
B3LYP/6-31G(d)	C_1	-656.1807873	0.258797	-655.958264	(0)
B3LYP/6-31+G(d,p)	C_1	-656.223446	0.257654	-656.002099	(0)
15^{2-}(s)					
B3LYP/6-31G(d)	C_1	-656.0498283	0.248740	-655.837842	75.6
B3LYP/6-31+G(d,p)	C_1	-656.13706	0.247232	-655.926797	47.3
15^{2-}(t)					
B3LYP/6-31G(d)	C_1	-656.0312338	0.248408	-655.820504	86.4
B3LYP/6-31+G(d,p)	C_1	-656.120833	0.247308	-655.911436	56.9